5-20-2011

L1 Adaptive Control of Uncertain Nonlinear Systems with Dynamic Constraints: As Applied to Commercial Aircraft Engines

Jennifer Hacker
Grauduate Student, jennifer.e.hacker@gmail.com

$\mathcal{L}_1$ Adaptive Control of Uncertain Nonlinear Systems with Dynamic Constraints: As Applied to Commercial Aircraft Engines

Jennifer Elizabeth Hacker

B.S., Purdue University, 2009

A Thesis
Submitted in Partial Fulfillment of the
Requirements for the Degree of
Master of Science
at the
University of Connecticut
2011

APPROVAL PAGE

Master of Science Thesis

$\mathcal{L}_1$ Adaptive Control of Uncertain Nonlinear Systems with Dynamic Constraints: As Applied to Commercial Aircraft Engines

Presented by

Jennifer Elizabeth Hacker, B.S. Mechanical Engineering

Major Advisor _____

Chengyu Cao

Associate Advisor _____

Robert Gao

Associate Advisor _____

Hanchen Huang

University of Connecticut

2011

ACKNOWLEDGEMENTS

I am grateful to the many people who have helped me learn and develop the knowledge needed to write this thesis. I would first like to sincerely thank my advisor, Professor Chengyu Cao, whose encouragement and guidance throughout my time in graduate school has enabled me to understand and develop $\mathcal{L}_1$ adaptive theory.

I would also like to thank my thesis committee members, Professor Hanchen Huang and Professor Robert Gao; without their time and assistance this thesis would not have been possible. I give thanks to Jim Fuller, Ten-Huei Guo, and Jonathan Litt for their work in engine control and for the guidance in helping with my understanding for aircraft engines.

Additionally, I would like to thank my colleagues: Jie Luo, Reza Sharifi, WeiDer Chung, Ali Elahidoost, Jiaxing Che, John Cooper, and Chuan Wang.

Finally, I give thanks to my family and friends whose support, love, and understanding has been an invaluable resource to me.

TABLE OF CONTENTS

TABLE OF FIGURES

ABSTRACT

This thesis presents the development and application of a $\mathcal{L}_1$ adaptive controller for a turbofan commercial aircraft engine in the presences of constraint limits. Turbofan engines are a highly complex system, with a wide variety of dynamics, operating under constantly changing environmental conditions. In aircraft turbofan operation many constraint requirements must be met. When constraints, such as rotor speeds, pressures, and temperatures, exceed the prescribed limits it can decrease the life expectancy of the engine, cause component failure, or even total engine failure. Additionally stall, also known as compressor surge, which occurs when the compressor is unable to work against incoming air resulting in flow reversal, must be avoided. To decrease the chances of entering into surge or stall, control systems are developed to control stall margin, which are percentage estimates of the probability that an engine will enter surge or stall. Overall, the control of a turbofan engine is a highly nonlinear problem that must be capable of handling variable constraints so an effective controller must be capable of handling nonlinearities while operation within constraints.

Despite the nonlinearity of the engine control problem, the aero-engine industry achieves engine control using linear design logic by creating several controls at different operating points and scheduling the resulting gains based on these different operating ranges. Therefore, this thesis proposes a $\mathcal{L}_1$ adaptive controller to handle nonlinear uncertain systems in the presence of constraint variables. These constraint variables are maintained through a dynamic integration limiter. $\mathcal{L}_1$ adaptive control theory permits transient characterization, deals with time varying uncertainties, and can create a tradeoff between tracking performance and robustness.

The theoretical foundation for the $\mathcal{L}_1$ adaptive controller is developed and analyzed, genetic simulations are conducted for the theoretical controller, as well as applying the controller to a Simulink model of a twin-spool commercial aircraft engine. Additionally, special consideration in placed on a stall margin estimator and used as a limiting variable. Simulation results are found to verify the theoretical findings.

1. Introduction

A. Background

The gas turbofan engine is the most common choice for modern aircraft propulsion in both industrial and military applications. Turbofan engines represent a highly complex system, with a wide variety of dynamics, operating under highly transient environmental conditions. A typical twin spool commercial turbofan engine can be seen below in Figure 1.

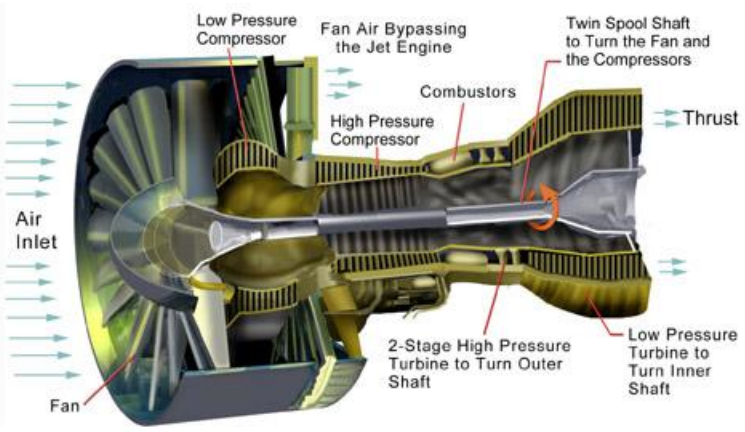

Figure 1: Twin Spool Turbo Fan Aircraft Engine

In a turbofan engine air enters the inlet, from the left in Figure 1, and passes through the fan. A fraction of the air is directed into the compressors, while the rest of the airflow is directed around the engine core and exits through the outer nozzle at the rear of the engine, known as bypass air. The airflow that is directed into the compressor goes through two compressor stages. The ingested air first passes through a low pressure compressor and then through a high pressure compressor. Both compressors are powered

by shafts driven off of the turbine. There is a twin spool shaft design, which allows high and low pressure sections of the engine to operate at different speeds, which is touched upon later. To sustain safe pressure levels inside the compressors, valves are generally present that can be opened to bleed air from the compressor. Additionally, stator vanes, geometric flow modulators, are often incorporated into the engine to direct airflow through the compressors. Upon exiting the high compressor the airflow enters the combustor, where fuel is added and ignited. After gaining large amounts of energy from the combustion process, the heated and pressurized air exits the combustor and transfers its kinetic energy to high and low pressure turbines. The high pressure turbine is connected to the outer part of the twin spooled shaft, often called the core rotor, and powers the high pressure compressor. The low pressure turbine powers the inner shaft, known as the fan rotor, which rotates the low pressure compressor and fan.

In aircraft turbofan engine operation many constraint requirements, such as rotor speeds, pressures, and temperatures, airflows, must be met. When constraints exceed the prescribed limits the life expectancy of an engine decreases, individual components may fail, ultimately resulting in total engine failure. In addition to these physical limits, the probability of entering a surge or stall becomes an important constraint factor during transient operation- acceleration and decelerations. Axi-symmetric stall, also known as compressor surge, happens when the compressor is unable to further compress or transport the already compressed incoming air, resulting in a reversal of airflow in the engine. This type of surge can lead to an expulsion of compressed heated air through the engine intake. When this occurs, the engine is unable to provide propulsion to the aircraft and engine components may become damaged, leading to failure. To decrease the

chances of entering into surge or stall, control systems are developed. A control variable, stall margin, is introduced as an estimation of the probability of the engine going into a stall. Stall margins are used as constraint factors in the turbofan engine control architecture. Therefore, not only does engine control need to have proper tracking performance, an example of tracking performance is systems response to throttle input, but it must do so while maintaining critical constraints.

Regulations created by the Federal Aviation Administration require aircraft engines to maintain set limits on temperature, pressure, shaft speed, and airflow, to ensure safe engine operation [1]. Current control systems are design to keep aircraft engines operating far from these set limits. Models are created of the turbofan engine under constant, normal operating conditions and control systems are designed around these models. It should be noted that often the imposed operation range greatly reduces the capabilities and efficiency of the engine.

In industry, for normal operation of the engines, control systems are designed with three basic function in mind; steady-state control, transient control, and limit protection control [2]. Steady-state control is a set-point control that is used to keep the engine operating at a desired point over time, such as idle, cruise, and take-off. This type of control is called a set-point control because it tries to control the engine to a "set-point", or fixed power level for the corresponding operating condition. Transient control and limit protection control are often coupled together in the control design, where transient control is developed to move from one engine steady-state operating point to another within in a given time frame and within prescribed bounds. To keep the engine from entering into unsafe or undesirable operating regions limit protection control is utilized.

Despite the nonlinearity of a gas turbine engine, linear control techniques are still the basis for the above mentioned controllers and use different forms of PID (proportional-integral-derivative) control[2].

However, after the linear control laws have been designed, some nonlinear control methods are added, such as gain scheduling. Gain scheduling achieves engine control by creating several controls at different operating points (i.e. varying altitudes, temperatures, and speeds) and scheduling the resulting gains, a gain is a constant of multiplication or amplification of a control signal, based on these different operating ranges [3-5]. The technique effectively "glues" a family of linear controllers into one large primary controller, which has the same structure as each individual set-point controller. The problem with gain schedule is there are an abundant number of combinations of operating conditions and creating such models is labor intensive.

These linear design controllers used in industry are robust to nonlinear uncertainties and capable of delivering good performance in normal operating situations. A control system is generally considered robust when it remains stable in the presence of variant conditions [6]. However, these controllers are designed to operate far from critical limits, often at the price of engine efficiency. A control system that allows for holding the necessary limits can be designed to operate more efficiently and closer to engine limits. Additionally in emergency situations, which will be discussed later, maintaining limits could prove to be very valuable [7]. However, maintaining limits is essentially a nonlinear requirement. Direct application of linear controllers generally results in poor performance. As an answer to this dilemma, control methods have been developed to

handle issues both, nonlinear dynamics and holding of critical limits, as discussed in the following section.

B. Constraint Control

An aircraft engine must maintain critical operating limits: pressures, temperatures, shaft speeds, airflows. During normal operation, most of these limits are not in danger of being surpassed. Constraint control demonstrates a benefit over conventional control when there is a need to operate near limits or to have active limit holding, as in the following cases.

Off-nominal/Emergency Situation

In 2006, a Bombardier Jet CRJ-100ER began take-off on the wrong runway. The runway was too short for take-off and as such the aircraft would not be able to achieve the needed thrust in time. Once the pilot realized his mistake the aircraft did not have sufficient runway to stop, and crashed after running off the runway [8]. Several runway incursions occur per year, where two planes have a "close call" on the runway. Achieving momentary levels of maximum thrust could be used to avoid crashes; whereas now this maximum thrust is well below the engine capabilities due to the PID control. These are examples illustrating a necessity for expanding operating limits closer to critical physical limits for emergency situations. Conventional linear systems must keep a large cushioning margin between physical limits and control limits to compensate for tracking of transient response. An intuitive solution to this problem is the introduction of a control system which is capable of holding constraints, expanding the operating range of the engine.

NASA's Resilient Propulsion Control Research for the NASA Integrated Resilient Aircraft Control (IRAC) Project [7] analyzed the benefits of achieving greater engine response in emergency situations. Normally, to achieve increased thrust in a turbofan engine, excessive fuel and airflow are required. However, if the airflow in the engine changes too rapidly, stall can occur; likewise, increased temperature/pressure can damage engine components and lead to total engine failure. This illustrates that constraint control could prove to be very beneficial in emergency situations, such as those investigated by NASA, when faster or greater thrust is needed.

Propulsion Flight Control

Vectorized engines manipulate the direction of the thrust created by the engine in order to control the altitude and velocity of the aircraft and provide superior maneuverability over conventional engines. Vectorized engines have recently been applied in military jet fighters, such as the F22 and F35, which require extreme maneuverability without compromising engine performance. Therefore the control systems implemented on such engines need to have complex constraint capabilities.

Also, industry is trending towards the merge of engine and flight control to form an integrated system. However, for the engine to serve as an effective actuator, such as aircraft control surfaces (rutter, wing flaps, etc), its magnitude (dynamic range of thrust) and bandwidth (how fast the magnitude can change) need to be increased significantly. In an integrated system, such as this where larger and fast response changes are needed, the output limits will frequently be encountered and will need to be actively maintained [2].

Higher efficiency Operation

Operation of an aircraft engine at points that lay far from the stall margin restricts the engine efficiency. The ‘peak point’, where the engine achieves the greatest fuel efficiency, lies on the stall margin limit line. This is a point of marginal stability meaning that the engine could go into stall any time without any precursor [4]. Operating close to the stall margin increases efficiency, while placing greater pressure on the control system to maintain the constraint. Conventionally, efficiency is compromised to maintain a safety margin from stall limits.

The above mentioned scenarios motivate a control theory which has the capabilities to ensure tracking performance while maintain various limits in the presence of significant uncertainties and nonlinearities. There are two methods currently used to handle constraints: optimal control and model predictive control.

Optimal control deals with constraints on either the input, unmeasured state, or output variables of the system while a performance objective is desired. When it comes to constrained control problems, optimal control methodology re-defines the problem into a discrete formulation, with a finite number of steps and constraints. Therefore the control signal can be found by solving the constrained optimization problem in real-time[9].

Model-Based Predictive Control (MPC) also know as receding horizon control technology [9] utilizes a mathematical model representation of the process. The algorithm evaluates multiple process inputs, predicts the direction of the desired control variable, and manipulates the output to minimize the difference between the target and actual variables. The method has been widely adopted in the process industry, for more than 30 years, as an effective means to deal with large multivariable constrained control

problems[10]. The main idea of MPC is to choose the control action by repeatedly solving an optimal control problem in real-time. Most MPC technologies are based on linear models, which are not ideal for highly nonlinear systems and could lead to poor performance.

In optimal and MPC control methods, a-priori knowledge of the system dynamics are required for the systems. In application, complex nonlinear dynamics are involved, such as those in a turbofan engine. Developing an accurate model would be extremely labor intensive, as dynamics of the system at many operating points must be recorded. Also, on an elementary level, developing precise knowledge of the uncertain time-varying system presents an immense challenge, both mathematically and practically.

Moreover, to maintain a constrained system is a transient requirement. Restricting a signal below a constant constraint is comparable to developing a response that has no overshoot, which is a transient specification in a tracking problem; as such the control system utilized in a constrained system should be analyzed for nonlinear systems, where transient performance is critical.

Therefore alternative constraint controls need to be developed. However, before developing an alternative constraint methodology, current forms of nonlinear control will be discussed.

C. Control of Nonlinear Uncertain Systems

The focus of this thesis is to develop a controller for nonlinear uncertain systems, namely a complex nonlinear turbofan system. Here I present a brief, but not all inclusive due to the breadth of research in this area, historical overview of control systems developed to handle nonlinear uncertain systems.

Since the late 1970's, sliding mode control (SMC) has generated much interest in the research community of nonlinear control [11]. SMC uses a high-frequency switching control method to switch from one continuous structure to another. Switching is based on the system's current position in state space; therefore SMC is considered a variable structure control method. The main advantage of SMC is its robustness to disturbances and insensitivity to parameter variations. The major problem with this method is the chattering effect, due to frequent mode switching, and danger of high-frequency oscillations of the controlled system [12].

Another control method widely investigated in the research community is nonlinear output feedback control with high gain observer. This method is capable of controlling a wide range of nonlinear systems by forcing the output feedback controller to improve the performance of the state feedback controller, if the gain of the observer output feedback controller is adequately high. The "Separation Principle" is the main reason for the use of a high gain observer in nonlinear output feedback control. The separation principle divides the system into an estimator or observer and a controller. The Separation Principle exists when the design of the state feedback controller is to be globally bounded [13].

Adaptive control is the final control methodology to be discussed, and is the focus of this thesis. Adaptive control is classified two ways "direct", which updates controller parameters, and "indirect", which updates plant parameters. There is also distinction between "Lyapunov-based" and "estimation-based" adaptive control. The classification difference between Lyapunov and estimation based schemes is that in the former, Lyapunov methodology is used to prove stability and convergence and the latter uses

least-square optimization algorithms [14]. Adaptive control has a variety of different branches, a few of them are described below.

Neural networks are adaptive control architectures modeled after biological neuron structures. Neural networks are designed to take advantage of distributed information processing, offering potential for parallel computing [15] . Copying the ability of the human cerebellum, which is able to "rewire" its neural networking to learn, neural network control makes decisions based on knowledge of other models and constant controller adaptation as dynamics of the unknown system are discovered.

Fuzzy logic adaptive control is based on the fuzzy logic mathematics, introduced in 1965 by Zadeh, which is a form of artificial intelligence. Fuzzy logic has been applied to nonlinear systems, which lack complete analytical models by utilizing a-priori knowledge of the system dynamic. Fuzzy logic is based on making decisions, conditional propositions, based on past knowledge. The dynamics of a system can be constructed from knowledge of similar systems using fuzzy logic arguments, and a fuzzy controller can be constructed via conditional proposition decisions [16].

Developed in 1961 by Whitaker and his group [17], model reference adaptive control (MRAC) is a direct approach that ensures asymptotic tracking of a desired a-priori defined reference model for a class of systems with constant unknown parameters. MRAC updates the parameters of the controller by comparing the response of the real system to the ideal response of a reference model, similar to the real system. MRAC has shown to be effective in aerospace applications, including the NASA genetic transport model (GTM) [18]. Moreover, adaptive control has been shown to be a versatile and

commonly accepted method for solving nonlinear control problems and nonlinear adaptive control will be the main focus of this thesis.

D. Adaptive Control of Nonlinear Uncertain Systems with Output Constraints

Despite the vast improvements in adaptive control design methods, they have largely remained a tool for adapting to slowly varying uncertainties, and the characterization of the transient phase is missing. Adaptive controllers and adaptation laws, in general, are derived using Lyapunov tools which offer no means for characterizing a system's input/output performance during the transient period. Transient performance is always critical in real world applications. The historical crash of X-15A-3 on November 15, 1967 and the resulting death of pilot Michael Adams were due to deficiencies of the stable, albeit non-robust, adaptive flight control system [19].

The transient performance of adaptive controllers changes drastically with modification to adaptive gains, reference inputs, initial conditions, and values of uncertain coefficients. The highly nonlinear dependence between these parameters, introduced via the adaptive laws, makes the theoretical analysis of the transient performance and stability margins extremely difficult. A set of design parameters with acceptable transient performance for one reference input may lead to a very poor transient for another reference input, or even lead to instability. Previous improvements of the transient performance of adaptive controllers has been achieved either at the price of oscillations in the adaptive control signal or high-gain feedback, which impedes the robustness [20].

In addition to undesired transient performance, for example control signals of high-frequency, large transient errors, or slow convergence rate of tracking errors, another

deficiency in conventional adaptive control is its inability to deal with time-varying uncertainties and, as previously mentioned, constraint control in a turbofan aircraft engine is highly nonlinear and time-varying.

Recently, a new variant of adaptive control, $\mathcal{L}_1$ adaptive control, has been developed. Utilizing fast and robust adaptation it permits transient analysis even for time varying uncertainties and is capable of handling constraints. Therefore $\mathcal{L}_1$ adaptive control is proposed as an adaptive approach for nonlinear time varying systems in the presence of state constraints.

E. $\mathcal{L}_1$ Adaptive Control

Over the past few years, $\mathcal{L}_1$ adaptive control theory has come to the foreground of controls research. It permits transient characterization, deals with time varying uncertainties, and can create a tradeoff between tracking performance and robustness [20-29]. $\mathcal{L}_1$ adaptive control theory allows for decoupling of adaption from robustness. The architecture also allows for transient characterization and robustness in the presence of fast adaptation without using persistent excitation, applying gain scheduling, or using high-gain feedback.

$\mathcal{L}_1$ adaptive control is a piece-wise continuous adaptive control that achieves the above mentioned goals by using three distinct laws. First, a state predictor law is used to model the system's desired performance. Concurrently, an adaption law ensures the plant and state estimates are identical. Finally, a control law utilizes a low pass linear filter to eliminate chatter in the control channel. To handle state constraints the proposed $\mathcal{L}_1$ adaptive controller uses an integration logic to switch between the control state and the limited states. When no signals need to be limited, the adaptive controller places priority

solely on the control channel. If a signal must be kept within limits, the controller switches priority to the limit channel. Moreover , $\mathcal{L}_1$ adaptive control can be used for nonlinear time varying systems in the presence of state constraints.

In addition to being able to handle nonlinear constrained systems, fast adaptation is also one of the main benefits of $\mathcal{L}_1$ control theory [20]. $\mathcal{L}_1$ control could be implemented to achieve faster engine response compared with the conventional methods currently utilized and previous research [3, 7, 30] has analyzed the benefits of achieving greater engine response in emergency situations.

An incident occurred in 1989 when a McDonnell Douglas DC-10, United Airlines flight 232, suffered an uncontained engine failure causing pieces from the engine to hit and destroy part of the tail and the horizontal stabilizer. As a result, all three of the hydraulic lines were cut, causing a complete loss of hydraulic fluid, disabling the flight control surfaces (i.e., ailerons, rudder, and all other flaps used to steer and control speed of the aircraft). The pilots then used the wing-mounted engines to steer the plane, using differential thrust to turn, and using additional or less thrust to control altitude. To some extent, the pilots were able to control the aircraft with properly timed changes in thrust. However, the engine response had time delays of as much as 20 to 40 seconds. Upon approach, the pilots found it was difficult to stay lined up with the runway or achieve an acceptable landing speed. The plane crash landed, killing 111 of the 296 on board [31]. In this case, a control system that allowed for faster engine response, such as $\mathcal{L}_1$ adaptive control, would have allowed the pilots to use the engines to steer more effectively and could have prevented the crash and resulting deaths.

Finally, the $\mathcal{L}_1$ controller has already been shown to be beneficial in other applications and proven to provide fast adaptation with guaranteed transients in a large variety of systems. $\mathcal{L}_1$ has been successfully demonstrated on drilling systems [32], wing rock [33], and other flight control systems [34]. Additionally, $\mathcal{L}_1$ adaptive control has been successful tested on NASA's AirSTAR test vehicle. The AirSTAR is a commercial twin-engine aircraft, dynamically-scaled to 5.5 percent of an actual aircraft. On June 2nd 2010, a test flight of the AirSTAR was preformed with an all-adaptive $\mathcal{L}_1$ flight control system in Fort Pickett, Va. The flight test with the $\mathcal{L}_1$ adaptive flight control system lasted approximately 14 minutes, completing a set of 14 flight cards, which are potentially dangerous situations an aircraft can encounter during a flight. The adaptive controller guaranteed safe operation of the vehicle during the flight, and the pilot satisfactorily flew the specified tasks [35].

This thesis presents an adaptive controller for turbofan engines, extending the results of [26] to develop an $\mathcal{L}_1$ adaptive controller for uncertain nonlinear systems with state constraints. The problem will be approached theoretically, simulated for generic systems with state constraints, and then the $\mathcal{L}_1$ adaptive controller will be applied to a model of a commercial gas turbine turbofan engine.

Chapter 2 states preliminary definitions, while Chapter 3 formulates the control problem. In Chapter 4, $\mathcal{L}_1$ adaptive control architecture is presented. Chapter 5 shows the analysis and theoretical proofs of the adaptive controller. Simulations are generated in Chapter 6, and the controller is applied to an engine model in Chapter 7. The thesis is concluded in Chapter 8, with simulation diagrams in the appendix.

Throughout this thesis, I indicates the identity matrix of appropriate dimension, $\|H(s)\|_{\mathcal{L}_1}$ denotes the $\mathcal{L}_1$ gain of $H(s)$, $\|x\|_{\mathcal{L}_\infty}$ denotes the $\mathcal{L}_\infty$ norm of $x(t)$, $\|x_t\|_{\mathcal{L}_\infty}$ denotes the truncated $\mathcal{L}_\infty$ norm of $x(t)$ at the time instant t, and $\|x\|_2$ and $\|x\|_\infty$ indicate the 2-and ∞- norms of the vector x respectively.

2. Preliminaries

In this section, I recall some basic definitions from linear system theory, using the single-input single-output (SISO) linear time-variant (LTV) system:

$$\dot{x}(t) = A(t)x(t) + B(t)u(t), \qquad x(0) = x_0, \tag{1}$$

where $A(t) \in \mathbb{R},\ B(t) \in \mathbb{R}$.

Definition 1. The system in (1) is *uniformly bounded-input, bounded-output (BIBO) stable*, if there exists a positive constant $\boldsymbol{a} > 0$ such that for any $\boldsymbol{t_0}$ and any bounded input signal $\boldsymbol{x(t)}$, the corresponding response for $\boldsymbol{x(0) = x_0}$ satisfies

$$\sup_{t \geq t_0} \|x(t)\|_\infty \leq a \sup_{t \geq t_0} \|u(t)\|_\infty .$$

Definition 2. $\boldsymbol{\varepsilon_\tau(t)}$ is a truncation of $\boldsymbol{\varepsilon(t)}$ defined by

$$\varepsilon_\tau(t) = \begin{cases} \varepsilon(t), & 0 \leq t \leq \tau \\ 0, & t > \tau \end{cases} \tag{2}$$

Definition 3. *The $\mathcal{L}_1$ norm of the SISO LTV system* in (1) is defined as

$$\|\mathcal{X}\|_{\mathcal{L}_1} \triangleq \sup_{t > \tau, \tau \in \mathbb{R}^+} \int_\tau^t |h(t,r)| dr, \tag{3}$$

where $\mathcal{X}$ is a map of the system, and $h(t,r)$ is the impulse response.

Definition 4. For a signal $\xi(t) = [\xi_1(t), \dots, \xi_n(t)]^T, t \geq 0$, its $\mathcal{L}_\infty$ norm and truncated $\mathcal{L}_\infty$ norm are defined respectively as

$$\|\xi\|_{\mathcal{L}_\infty} = \max_{i=1,\dots,n} (\sup_{\tau \geq 0} |\xi_i(\tau)|),$$

$$\|\xi_t\|_{\mathcal{L}_\infty} = \max_{i=1,\dots,n} (\sup_{0 \leq \tau \leq t} |\xi_i(\tau)|)$$

(4)

Definition 5. First Order ODE Solution [36]: For the system in (1), a solution can be found in the following form:

$$x(t) = e^{-\int A(t)dt} \left(\int e^{\int A(\tau)d\tau} B(t)u(t)dt + c \right)$$

(5)

where c is a constant which depends on the initial condition x_0.

3. Problem Formulation

In this section, the theoretical problem formulation is developed. First, consider the following system:

$$\dot{x}(t) = f(x(t), u(t), t), \qquad x(0) = x_0, \tag{6}$$

$$\dot{p}_i(t) = g_i(p_i(t), u(t), t), \qquad p_{i_{min}} < p_i(0) < p_{i_{max}}, \tag{7}$$

where $i = (1,2, \dots, n)$, $x(t) \in \mathbb{R}$ is the system's state variable to be controlled, $p_i(t) \in \mathbb{R}$ is the system's i^{th} variable to be constrained, f and g_i are an unknown nonlinear function, and $u(t) \in \mathbb{R}$ is the input control signal. p_L and p_U are the system's lower and upper bounds, respectively and can be calculated accordingly: $p_L = max_{i=1}^{n}(p_{i_{min}})$ and $p_U = min_{i=1}^{n}(p_{i_{max}})$. **The control objective is to track $\boldsymbol{x(t)}$ while keeping each $\boldsymbol{p_i(t)}$ in the set bounds $\boldsymbol{p_{i_{min}} < p_i(t) < p_{i_{max}}}$.** Additionally, a reference command $r(t) \in \mathbb{R}$ is passed through the system input $u(t)$ for $x(t)$ to follow. We make the following assumptions about the system outlined above:

Assumption 1: *Semiglobal Lipschitz condition*. For any $\delta > 0$, there exists a positive $K(\delta) > 0$ and $B > 0$ such that

$$\|g(p_1, u, t) - g(p_2, u, t)\|_\infty \leq K(\delta)\|p_1 - p_2\|_\infty$$

$$\|g(0, u, t)\|_\infty \leq B \tag{8}$$

for all $\|p_1\|_\infty \leq \delta$ and $\|p_2\|_\infty \leq \delta$ uniformly in t.

Assumption 2: *Known sign of Control Effectiveness*. There exist upper and lower bounds $\lambda_u > \lambda_l > 0$ and $\theta_u > \theta_l > 0$ such that

$$\lambda_l \leq \frac{\partial f(x,u,t)}{\partial u} \leq \lambda_u,\ \theta_l \leq \frac{\partial g(p,u,t)}{\partial u} \leq \theta_u. \tag{9}$$

Assumption 3: *Semiglobal uniform boundedness of partial derivatives*. For any $\rho_{p_i}, \rho_u > 0$, there exists positive $b_{g_{p_i}}(\rho_{p_i}, \rho_u) > 0$ and $b_{g_{i_t}}(\rho_{p_i}, \rho_u) > 0$, such that for any $\|p_i(t)\|_\infty \leq \rho_{p_i}$ and $\|u(t)\|_\infty \leq \rho_u$ the partial derivatives of $g_i(p_i(t), u(t), t)$ are piece-wise continuous and bounded:

$$\left\|\frac{\partial g_i(p_i,u,t)}{\partial p_i}\right\| \leq b_{g_{p_i}}(\rho_{p_i}, \rho_u), \left\|\frac{\partial g_i(p_i,u,t)}{\partial t}\right\| \leq b_{g_{i_t}}(\rho_{p_i}, \rho_u) \tag{10}$$

Assumption 4: If $p_i(t)$ is bounded, then $x(t)$ is bounded.

Remark: Note that Assumptions 1-3 are typical in adaptive control theory. Assumption 4 typically holds true in practical applications.

Therefore to develop the mathematic framework for the $\mathcal{L}_1$ adaptive controller we reformulate the system in (6)-(7) as:

$$\dot{x}(t) = A_x x(t) + B_x u(t) + \sigma_x(t), \tag{11}$$

$$\sigma_x(t) = f(x(t), u(t), t) - A_x x(t) - B_x u(t), \tag{12}$$

$$\dot{p}_i(t) = A_{p_i} p_i(t) + B_{p_i} u(t) + \sigma_{p_i}(t),$$

(13)

$$\sigma_{p_i}(t) = g_i(p_i(t), u(t), t) - A_{p_i} p_i(t) - B_{p_i} u(t).$$

(14)

where $i = (1,2, \dots, n)$, A_x and A_{p_i} are negative constants, B_x and B_{p_i} are positive constants, and $\sigma_x(t)$ and $\sigma_{p_i}(t)$ are the unmodeled dynamics. Again the control objective is to track $x(t)$ while keeping each $p_i(t)$ in the set bounds:

$$p_{i_{min}} < p_i(t) < p_{i_{max}}.$$

(15)

4. $\mathcal{L}_1$ Adaptive Control Architecture

In this section, I present the architecture of the $\mathcal{L}_1$ adaptive controller. Figure 2 is the block diagram representation of the general structure of the adaptive controller. The three main components are the state predictor, the adaptive law, and the control law. These components are described further in the following text. Additionally, for each of these components there are separate divisions for the $x(t)$ and $p(t)$ channels.

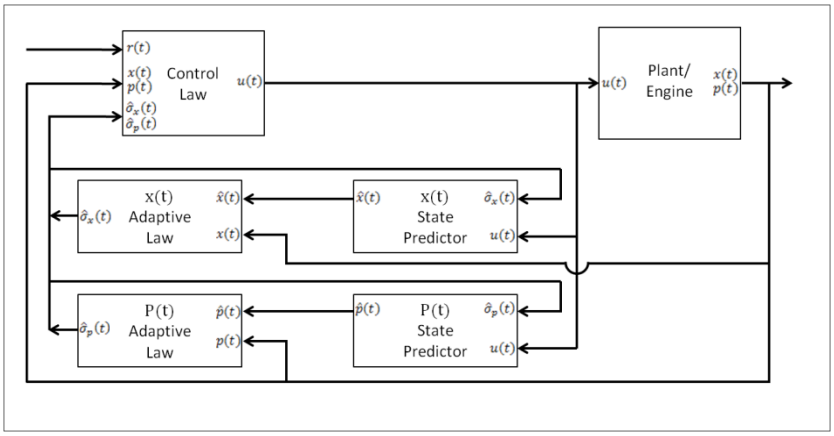

Figure 2: $\mathcal{L}_1$ Adaptive Control Architecture

Note that Figure 2 shows only the general structure for a single constraint system, however this paper aims to analyze multiple constraint cases. Therefore for every limiting factor in the system there will be an additional control law, adaptive law and state predictor for each respective $p_i(t)$ signal.

The $\mathcal{L}_1$ adaptive controller uses a state predictor to create reference models with desired system dynamics. Next, the state predictor's reference system signal, as well as the plant's response, are fed into the adaptive law, which generates new controller parameters that are incorporated into the control law. The control law will create different control signals, $u_i(t)$, that correspond to $x(t)$ and each $p_i(t)$, and, through a low pass filter and a dynamic limit integrator, will produce a control signal, $u(t)$ based upon the condition of each limit. The following develops the three components in greater detail.

State Predictor: The state predictor is comprised of two parts, with $x(t)$ and $p_i(t)$ models similar to (11)-(14):

$$\dot{\hat{x}}(t) = A_x\hat{x}(t) + B_x u(t) + \hat{\sigma}_x(t), \qquad \hat{x}(0) = x(0), \tag{16}$$

$$\dot{\hat{p}}_i(t) = A_{p_i}\hat{p}_i(t) + B_{p_i} u(t) + \hat{\sigma}_{p_i}(t), \qquad \hat{p}_i(0) = p_i(0), \tag{17}$$

where $i = (1,2,\dots,n)$, A_x and A_{p_i} are negative constants, B_x and B_{p_i} are positive constants, and $\hat{\sigma}_x(t)$ and $\hat{\sigma}_{p_i}(t)$ are estimates of the unmodeled dynamics, found using the adaptive law. The parameters A_x, A_{p_i}, B_x, and B_{p_i} can be selected to give the system the desired dynamics, while $\hat{\sigma}_x(t)$ and $\hat{\sigma}_{p_i}(t)$ ensure that $\hat{x}(t)$ is almost identical to $x(t)$.

Adaptive Law: The adaptive estimates $\hat{\sigma}_x(t)$ and $\hat{\sigma}_{p_i}(t)$ are piece-wise continuous and are given by

$$\hat{\sigma}_x(t) = \hat{\sigma}_x(jT), t \in [jT, (j+1)T), \tag{18}$$

$$\hat{\sigma}_x(jT) = -\left(\int_0^T e^{A_x(T-\tau)d\tau}\right)^{-1} e^{A_x T}\tilde{x}(jT),$$

(19)

$$\hat{\sigma}_{p_i}(t) = \hat{\sigma}_{p_i}(jT), t \in [jT, (j+1)T),$$

(20)

$$\hat{\sigma}_{p_i}(jT) = -\left(\int_0^T e^{A_{p_i}(T-\tau)d\tau}\right)^{-1} e^{A_{p_i} T}\tilde{P}(jT),$$

(21)

where $j = 0,1,2,...$, and the error is $\tilde{x}(t) = \hat{x}(t) - x(t)$ and $\tilde{p}_i(t) = \hat{p}_i(t) - p_i(t)$, while T is the signal sampling rate. Decreasing the sampling rate T, used by the adaptive controller, decreases the errors $\tilde{x}(t)$ and $\tilde{p}_i(t)$.

Control Law: To develop the control law, consider the switching logic utilized. If all $p_i(t)$ signals are within their respective bounds, the control law for $u(t)$ to control $x(t)$ is typical [20]:

$$u(s) = u_x(s) = -C(s)\frac{\hat{\sigma}_x(s) + A_x r(s)}{B_x},$$

(22)

where the first order filter, $C(s) = \frac{\omega}{s+\omega}$ and ω is a constant. When a $p_i(t)$ arrives at its the preset limits, for example $p_i(t) = p_{i_{max}}$, the system should not simply switch to $u(s) = u_p(s) = -C(s)\frac{\hat{\sigma}_{p_i}(s) + A_{p_i}\hat{p}_i(s)}{B_{p_i}}$ to maintain $p_i(t) = p_{i_{max}}$. If this were the case, there exists no exiting mechanism to switch back to the nominal mode and $u(t)$ is always

used to control $p_i(t)$ to stay at $p_{i_{max}}(t)$. Therefore, to achieve limit holding, the control law incorporates an integrator with dynamic constraints and takes the form:

$$u(t) = \int_{u_L^*(t)}^{u_U^*(t)} -\omega \left(u(t) + \frac{\hat{\sigma}_x(t) + A_x r(t)}{B_x} \right) dt,$$

(23)

where ω is a gain constant. Also it should be noted, through the use of such integration the control signal is filtered.

To develop the integration bounds for the control signal the following are first defined:

$$u_{i_{max}}(t) = -\frac{\hat{\sigma}_{p_i}(t) + A_{p_i}\hat{p}_{i_{max}}}{B_{p_i}},$$

(24)

$$u_{i_{min}}(t) = -\frac{\hat{\sigma}_{p_i}(t) + A_{p_i}\hat{p}_{i_{min}}}{B_{p_i}},$$

(25)

where $\hat{p}_{i_{max}}$ and $\hat{p}_{i_{min}}$ are the upper and lower bounds for each $\hat{p}_i(t)$ output signal respectively and are defined as

$$\hat{p}_{i_{max}} = p_{i_{max}} - \bar{\gamma}_{p_i},$$

(26)

$$\hat{p}_{i_{min}} = p_{i_{min}} + \bar{\gamma}_{p_i}.$$

(27)

where $\bar{\gamma}_{p_i}$ is an arbitrary positive constant. Then, the integration bounds become

$$u_U(t) = min_{i=1}^{n}(u_{i_{max}}),$$

(28)

$$u_L(t) = max_{i=1}^{n}\left(u_{i_{min}}\right),$$

(29)

where $u_U(t)$ and $u_L(t)$ are the upper and lower bounds of the system's control signal. To ensure discontinuities are avoided, a smooth transition technique can be used such that

$$u^*_{i_{max}}(t) = u_{i_{max}}(t) + k\left(p_{i_{max}} - p_i\right),$$

(30)

$$u^*_{i_{min}}(t) = u_{i_{min}}(t) - k\left(p_i - p_{i_{min}}\right),$$

(31)

where k is chosen to be a large positive constant. Therefore the upper and lower integration bounds become

$$u^*_U(t) = min_{i=1}^{n}(u^*_{i_{max}}(t)),$$

(32)

$$u^*_L(t) = min_{i=1}^{n}\left(u^*_{i_{min}}(t)\right).$$

(33)

5. Analysis of $\mathcal{L}_1$ Adaptive Control

In this section the stability and performance of the proposed $\mathcal{L}_1$ controller are analyzed. For convenience, in the following proofs, p_i and u_i will be referred to as p and u respectively. It should be noted the following proofs hold for each p_i and u_i.

First, in order to analyze the proposed $\mathcal{L}_1$ controller the following variables are defined:

$$\eta_1(t) = e^{A_p t},$$

(34)

$$\eta_2(t) = -\int_0^t e^{A_p(t-\tau)} d\tau \left(\int_0^T e^{A_p(T-\tau)} d\tau \right)^{-1} e^{A_p T},$$

(35)

$$\eta_3(t) = \int_0^t e^{A_p(t-\tau)} d\tau,$$

(36)

$$\beta_1(T) = \max_{t\in[0,T]} |\eta_1(t)|,$$

(37)

$$\beta_2(T) = \max_{t\in[0,T]} |\eta_2(t)|,$$

(38)

$$\beta_3(T) = \max_{t\in[0,T]} |\eta_3(t)|.$$

(39)

Next, the following are defined

$$\zeta_p(T) = \left| \int_0^T e^{A_p(T-\tau)} d\tau \right| b_{\sigma_p},$$

(40)

$$\gamma_0(T) = \big(\beta_1(T) + \beta_2(T)\big)\zeta_p(T) + \beta_3(T) b_{\sigma_p},$$

(41)

where b_{σ_p} will be developed in Lemma 1.

Lemma 1: If the bounds

$$\|x_t\|_{\mathcal{L}_\infty} < \rho_x, \|p_t\|_{\mathcal{L}_\infty} < \rho_p, \|u_t\|_{\mathcal{L}_\infty} < \rho_u$$

(42)

exist, then there exists $b_{\sigma_p}(\rho_p, \rho_u)$, $b_{\sigma_x}(\rho_x, \rho_u)$, and $b_{d\sigma_p}(\rho_p, \rho_u)$ such that

$$\left\| (\sigma_p)_t \right\|_{\mathcal{L}_\infty} \leq b_{\sigma_p}(\rho_p, \rho_u),$$

(43)

$$\|(\sigma_x)_t\|_{\mathcal{L}_\infty} \leq b_{\sigma_x}(\rho_x, \rho_u)$$

(44)

$$\max_{t \in [jT, (j+1)T)} \left\| (\dot{\sigma}_p)_t \right\| \leq b_{d\sigma_p}(\rho_p, \rho_u),$$

(45)

where $\dot{\sigma}_p$ is piece-wise continuous and ρ_p and ρ_u are the prescribed bounds for p and u respectively.

Proof. It follows from Assumption 1, (**42**) that $g(p(t), u(t), t)$ is bounded and therefore $\sigma_p = g(p(t), u(t), t) - A_p p(t) - B_p u(t)$ is bounded, so without loss of generality, there exist $b_{\sigma_p}(\rho_p, \rho_u)$ such that (43) holds. From Assumption 4, if $\|p_t\|_{\mathcal{L}_\infty} < \rho_p$, then we

have $\|x_t\|_{\mathcal{L}_\infty} < \rho_x$. Similarily, from Assumption 1, there exists $b_{\sigma_x}(\rho_p, \rho_u)$ such that (44) holds.

Next, to prove there exists $\dot{\sigma}_p(t)$ and it is bounded for every time period $[jT, (j+1)T)$, we show that $\dot{u}(t)$ is bounded for each time period $[jT, (j+1)T)$. To prove $\dot{u}(t)$ is bounded, the four possible conditions of $\hat{p}(t)$ are analyzed

1. when $\hat{p}(t)$ is within the range $(\hat{p}_{min}, \hat{p}_{max})$,
2. when $\hat{p}(t) = \hat{p}_{max}$,
3. when $\hat{p}(t) = \hat{p}_{min}$,
4. and during the transition between the above three conditions.

First, when $\hat{p}(t)$ is within the range $(\hat{p}_{min}, \hat{p}_{max})$, it follows from the control law (**23**) that

$$\dot{u}(t) = -\omega\left(u(t) + \frac{\hat{\sigma}_x(t) + A_x r(t)}{B_x}\right) \tag{46}$$

Furthermore, it follows from the adaptive law (**19**) and Corollary 1, that $\hat{\sigma}_x$ is bounded. Also note that the reference signal $r(t)$ is bounded. Thus $\dot{u}(t)$ is bounded for each time period $[jT, (j+1)T)$, if $\|p_t\|_{\mathcal{L}_\infty} < \rho_p$, $\|u_t\|_{\mathcal{L}_\infty} < \rho_u$, and $\hat{p}(t) \in (\hat{p}_{min}, \hat{p}_{max})$.

Second, when $\hat{p}(t) = \hat{p}_{max}$, then $u(t) = -\frac{\hat{\sigma}_p(t) + A_p \hat{p}_{max}}{B_p}$. Since $\hat{p}_{max}$ is constant and $\hat{\sigma}_p(t)$ is continuous for each time period $[jT, (j+1)T)$, $\dot{u}(t)$ exists and is:

$$\dot{u}(t) = -\frac{\dot{\hat{\sigma}}_p(t) + A_p \dot{\hat{p}}_{max}}{B_p}$$

$$= -\frac{\dot{\hat{\sigma}}_p(t)}{B_p}.$$

(47)

Note that $\dot{\tilde{p}}(t) = \dot{p}(t) - \dot{\hat{p}}(t)$. So when $\hat{p}(t) = \hat{p}_{max}$, then $u(t) = -\frac{\hat{\sigma}_p(t) + A_p \hat{p}_{max}}{B_p}$ which makes $\dot{\hat{p}}(t) = 0$. It follows from (43) that $\dot{p}(t) = A_p p(t) + B_p u(t) + \sigma_p(t)$ is bounded, if $\|p_t\|_{\mathcal{L}_\infty} < \rho_p$ and $\|u_t\|_{\mathcal{L}_\infty} < \rho_u$, which implies $\dot{\tilde{p}}(t)$ is bounded for each time period $[jT, (j+1)T)$. Thus $\dot{u}(t)$ is bounded for each time period $[jT, (j+1)T)$, when $\hat{p}(t) = \hat{p}_{max}$, if $\|p_t\|_{\mathcal{L}_\infty} < \rho_p$, $\|u_t\|_{\mathcal{L}_\infty} < \rho_u$. Third, when $\hat{p}(t) = \hat{p}_{min}$, similarly $\dot{u}(t)$ is also found to be bounded during that time period.

Fourth, since equation (**30**) and (**31**) ensure a smooth transition which avoids discontinuities, $\dot{u}(t)$ is bounded during the transition. Therefore, from the above discussion we can conclude that $\dot{u}(t)$ is bounded for the four conditions of $\hat{p}(t)$ for each time period $[jT, (j+1)T)$, if $\|p_t\|_{\mathcal{L}_\infty} < \rho_p$ and $\|u_t\|_{\mathcal{L}_\infty} < \rho_u$.

Since $\sigma_p(t) = g(p(t), u(t), t) - A_p p(t) - B_p u(t)$ and its derivatives exists, for each $[jT, (j+1)T)$ then

$$\dot{\sigma}_p(t) = \frac{\partial g}{\partial p}\dot{p}(t) + \frac{\partial g}{\partial u}\dot{u}(t) + \frac{\partial g}{\partial t} - A_p \dot{p}(t) - B_p \dot{u}(t), \qquad t \in [jT, (j+1)T).$$

(48)

It follows from Assumption 2 and 3 that $\dot{p}(t)$ is bounded, and from above $\dot{u}(t)$ is bounded and $\dot{\sigma}_p(t)$ is also bounded for each time period $[jT, (j+1)T)$, so without loss of generality, there exists $b_{d\sigma_p}(\rho_p, \rho_u)$ such that (**45**) if (**42**) holds.

This concludes the proof of Lemma 1. □

Lemma 2:

$$\lim_{T\to 0} \gamma_0(T) = 0.$$

(49)

Proof. Since b_{σ_p} is bounded and using (**40**), it can be shown that

$$\lim_{T\to 0} \zeta_p(T) = 0,$$

(50)

From (**37**)

$$\lim_{T\to 0} \beta_1(T) = \lim_{t\to 0} |\eta_1(t)| = 1.$$

and from (**38**)

$$\lim_{T\to 0} \beta_2(T) = \lim_{t\to 0} |\eta_2(t)| = -1.$$

Therefore β_1 and β_2 and bounded.

From (**39**) it is seen

$$\lim_{T\to 0} \beta_3(T) = \lim_{t\to 0} |\eta_3(t)| = 0.$$

(51)

Since $b_{d\sigma_p}$ is bounded and using (**50**) and (**51**)

$$\lim_{T\to 0} \gamma_0(T) = 0.$$

(52)

This concludes the proof of Lemma 2. □

Next, the following is defined. For any given positive $\bar{\gamma}_p$ and $\bar{\gamma}_{\sigma_p}$ choose T such that the following is true

$$\gamma_0(T) < \bar{\gamma}_p$$

(53)

$$\left|A_p\right|\bar{\gamma}_p + b_{d\sigma_p}\ T < \bar{\gamma}_{\sigma_p}$$

(54)

Lemma 3: Given the system dynamics in (**13**) and $\mathcal{L}_1$ adaptive controller developed in Section 4, if

$$\|p_t\|_{\mathcal{L}_\infty} < \rho_p, \|u_t\|_{\mathcal{L}_\infty} < \rho_u$$

(55)

and T is chosen to ensure (**53**) and (**54**) hold, then

$$\|\tilde{p}_t\|_{\mathcal{L}_\infty} < \bar{\gamma}_p$$

(56)

$$\|\left(\hat{\sigma}_p - \sigma_p\right)_t\|_{\mathcal{L}_\infty} < \bar{\gamma}_{\sigma_p}$$

(57)

where $\bar{\gamma}_p$ and $\bar{\gamma}_{\sigma_p}$ are defined in (**53**) and (**54**) and ρ_p and ρ_u are the prescribed bounds for p and u respectively.

Proof. We prove (**56**) by a contradiction argument. Since $\tilde{p}(0) = 0$ and $\tilde{p}(t)$ is continuous, where $\tilde{p}(t) = \hat{p}(t) - p(t)$ then assume there exists a t' such that

$$|\tilde{p}(t')| = \bar{\gamma}_p$$

(58)

which leads to

$$\|\tilde{p}_{t'}\|_{L_\infty} \leq \bar{\gamma}_p$$

(59)

Since $\tilde{p}(t) = \hat{p}(t) - p(t)$ and using (**13**) and (**17**), then

$$\dot{\tilde{p}}(t) = A_p\tilde{p}(t) + \hat{\sigma}_p(t) - \sigma_p(t)$$

(60)

Then,

$$\tilde{p}((j+1)T) = e^{A_pT}\tilde{p}(jT) + \int_0^T e^{A_p(T-\tau)}\hat{\sigma}_p(jT)d\tau - \int_0^T e^{A_p(T-\tau)}\sigma_p(jT+\tau)\,d\tau$$

where $j = 0,1,2,\ldots$ Next, substitution of adaptive law (**21**) into above equation yields

$$\tilde{p}((j+1)T) = -\int_0^T e^{A_p(T-\tau)}\sigma_p(jT+\tau)\,d\tau$$

(61)

So

$$\left|\tilde{p}\big((i+1)T\big)\right| \le \left|\int_0^T e^{A_p(T-\tau)}d\tau\right| b_{\sigma_p}$$

$$\le \zeta_p(T), \qquad jT \le t'$$

(62)

For all $jT + t \le t'$,where $t \in [0, T]$, then

$$\tilde{p}(jT+t) = e^{A_pt}\tilde{p}(jT) + \int_0^t e^{A_p(t-\tau)}\hat{\sigma}_p(jT)d\tau - \int_0^t e^{A_p(t-\tau)}\sigma_p(jT+\tau)\,d\tau.$$

(63)

Using equations (**34**)-(**36**) and (**63**), it is found that

$$\tilde{p}(jT+t) \le \eta_1(t)\tilde{p}(jT) + \eta_2(t)\tilde{p}(jT) + \eta_3(t)b_{\sigma_p.}$$

(64)

Then using (**64**), the following is found

$$|\tilde{p}(jT+t)| \le |\eta_1(t)||\tilde{p}(jT)| + |\eta_2(t)||\tilde{p}(jT)| + |\eta_3(t)|b_{\sigma_p}$$

(65)

From (**37**)-(**39**), and (**62**), (**65**) becomes

$$|\tilde{p}(jT+t)| \leq \big(\beta_1(T)+\beta_2(T)\big)\zeta_p(T)+\beta_3(T)b_{\sigma_p}.$$

(66)

From the definition in (**41**),

$$|\tilde{p}(jT+t)| \leq \gamma_0(T).$$

(67)

Then for all $t \in [0, t']$, we have

$$|\tilde{p}(t)| \leq \bar{\gamma}_0(T),$$

(68)

along with the assumptions on T introduced in (**45**) yields

$$\|\tilde{p}_{t'}\|_{\mathcal{L}_\infty} < \bar{\gamma}_p.$$

(69)

which contradicts (**59**). Therefore $\|\tilde{p}_t\|_{\mathcal{L}_\infty} < \bar{\gamma}_p$.

Next I prove (**57**). According to the adaption law in (**20**) and (**21**), we have

$$\left(\int_{jT}^{(j+1)T} e^{A_p\left((j+1)T-\tau\right)}d\tau\right)\hat{\sigma}_p(jT)+e^{A_pT}\tilde{p}(jT)=0.$$

(70)

From (**61**)

$$\tilde{p}((j+1)T) = -\int_{jT}^{(j+1)T} e^{A_p\left((j+1)T-\tau\right)}\sigma_p(\tau)\,d\tau.$$

(71)

From (**70**)

$$\tilde{p}(jT) = (I - e^{A_p T})\tilde{p}(jT) - \int_{jT}^{(j+1)T} e^{A_p((j+1)T-\tau)}\hat{\sigma}_p(jT)d\tau$$

$$= -\int_{jT}^{(j+1)T} e^{A_p((j+1)T-\tau)}\left(\hat{\sigma}_p(jT) + A_p\tilde{p}(jT)\right)d\tau$$

(72)

$$\tilde{p}((j+1)T) = -\int_{(j+1)T}^{(j+2)T} e^{A_p((j+2)T-\tau)}\left(\hat{\sigma}_p\big((j+1)T\big) + A_p\tilde{p}\big((j+1)T\big)\right)d\tau$$

(73)

It follows from (**71**) and (**73**)

$$-\int_{jT}^{(j+1)T} e^{A_p((j+1)T-\tau)}\sigma_p(\tau)\,d\tau$$

$$= -\int_{(j+1)T}^{(j+2)T} e^{A_p((j+2)T-\tau)}\left(\hat{\sigma}_p\big((j+1)T\big) + A_p\tilde{p}\big((j+1)T\big)\right)d\tau$$

(74)

Thus, from the mean value theorem for integration [15], there exists $t_p \in [jT, (j+1)T)$, such that

$$\sigma_p(t_p) = \hat{\sigma}_p(jT) + A_p\tilde{p}(jT).$$

(75)

For any t, which can always be considered within $[jT, (j+1)T)$, there exist $t_p \in [jT, (j+1)T)$, such that $|t - t_p| < T$,

$$\|\hat{\sigma}_p(t) - \sigma_p(t)\| = \|\hat{\sigma}_p(jT) - \sigma_p(t)\|$$

$$\leq \|\hat{\sigma}_p(jT) - \sigma_p(t_p)\| + \|\sigma_p(t) - \sigma_p(t_p)\|$$

$$\leq \left|A_p\right|\left|\tilde{p}(jT)\right| + \int_{t_p}^{t} \left\|\dot{\sigma}(\tau)\right\| d\tau$$

(76)

Note that (**76**) only requires $\dot{\sigma}(\tau)$ exist for each time period $[jT, (j+1)T)$. Since $\left\|\dot{\sigma}(\tau)\right\| \leq b_{d\sigma_p}$ is bounded for each $\tau \in [jT, (j+1)T)$. in (**45**), then

$$\left\|\hat{\sigma}_p(t) - \sigma_p(t)\right\| \leq \left|A_p\right|\bar{\gamma}_p + b_{d\sigma_p}\ T < \bar{\gamma}_{\sigma_p}$$

(77)

Therefore (**57**) is proven. This concludes the proof of Lemma 3. □

Corollary 1: Using the same method as above, it can also be shown that if

$$\|x_t\|_{\mathcal{L}_\infty} < \rho_x,$$

(78)

and T is chosen to ensure

$$\gamma_1(T) < \bar{\gamma}_x$$

(79)

hold, then

$$\|\tilde{x}_t\|_{\mathcal{L}_\infty} < \bar{\gamma}_x$$

(80)

□

Theorem 1. Consider the closed-loop system with the $\mathcal{L}_1$ adaptive controller developed in Section 4, if T is chosen such that (**53**) and (**54**) hold, we have

$$\hat{p}_{min} \leq \hat{p}(t) \leq \hat{p}_{max},$$

(81)

$$p_{min} < p(t) < p_{max},$$

(82)

where $\hat{p}_{min}$ and $\hat{p}_{max}$ are defined in (**26**) and (**27**).

Proof. Again a contradiction method will be used to prove (**81**). Since $\hat{p}_{min} \leq \hat{p}(0) \leq \hat{p}_{max}$, and $\hat{p}(t)$ is continuous, and if (**81**) is not true then there exists a t' such that

$$\hat{p}(t') = \hat{p}_{max} \tag{83}$$

and

$$\dot{\hat{p}}(t') > 0. \tag{84}$$

From the control law (**30**), we have

$$u^*_{max} = u_{max}(t') = -\frac{\hat{\sigma}_p(t') + A_p\hat{p}_{max}}{B_p} \tag{85}$$

where $\hat{p}_{max}$ is defined in (**26**) as $p_{max} - \bar{\gamma}_p$. Substituting (**85**) into the state predictor (**17**) and using (**83**), it is found that

$$\dot{\hat{p}}(t') = A_p\hat{p}(t') - A_p\hat{p}_{max} = A_p(\hat{p}(t') - \hat{p}_{max}) = 0. \tag{86}$$

Therefore, from the control law design (**23**)

$$u^*_{min}(t) \leq u(t) \leq u^*_{max}(t) \tag{87}$$

and it follows from Assumption 2 and (**86**) that

$$\dot{\hat{p}}(t') \leq 0, \text{for } u(t) \leq u^*_{max}(t). \tag{88}$$

Once $\hat{p}(t)$ reaches the upper bound $\hat{p}_{max}$, it will not exceed this upper bound since $\dot{\hat{p}}(t) \leq 0$. So it is seen that **(88)** contradicts (**84**).

Similarly, when $\hat{p}(t') = \hat{p}_{min}$, it is found that

$$\dot{\hat{p}}(t') \geq 0, \text{for } u(t) \geq u^*_{min}(t). \tag{89}$$

Therefore,

$$\hat{p}_{min} \leq \hat{p}(t) \leq \hat{p}_{max}. \tag{90}$$

From Lemma 3, we have $\|\tilde{p}_t\|_{\mathcal{L}_\infty} < \bar{\gamma}_p$, so using equation (**26**), (**27**), and (**90**) then

$$p_{min} < p(t) < p_{max} \tag{91}$$

which concludes the proof of Theorem 1. □

6. Simulations

To show the capabilities of $\mathcal{L}_1$ adaptive control, simulations are presented in this section. First, a simpler model is present that has only one limiting state. The second set of simulations presented is more complex and handles three limits.

A. Single Limit Simulations

For the single limit system the following system dynamics are used:

$$\dot{x}(t) = -x(t) + u(t) + 0.25\sin(2t) + 0.1,$$
$$\dot{p}(t) = -2p(t) + 16u(t) - 19.2\sin(1.8t + 2.3).$$

In order to show the controller maintains the bounds of the single state, $P(t)$, the limits are set at $p_{max} = 8$ and $p_{min} = 0$, the iteration time step is $T = 10^{-3}$seconds and the controller parameters are set as the follows:

$$A_x = -5, \qquad B_x = 1, \qquad A_p = -5, \qquad B_p = 1, \qquad \omega = 100.$$

Figure 3 shows the unconstraint x (solid green line) and the constrained x (solid blue line) tracking the reference command (dotted red line). Figure 4 shows the limited state p both when unconstrained (dashed green line) and constrained (solid blue line). The $\mathcal{L}_1$

adaptive controller is able to hold the single limit, $p(t)$ and the prescribed limits with some cost to the performance.

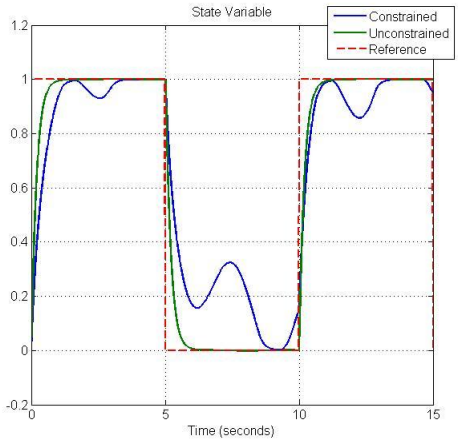

Figure 3: State $x(t)$, limited (blue), and unlimited (green)

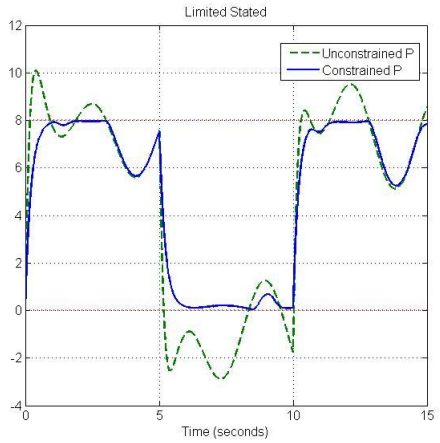

Figure 4: Limited $p(t)$, limited (blue), and unlimited (green dashed)

B. Multiple Limit Simulations

The next set of simulation shows a more complex system with three limiting states. The dynamics of this system are:

$$\dot{x}(t) = -3x(t) + u(t) + 0.5\sin(2t) + \begin{bmatrix} 1 \\ 0.5 \end{bmatrix} z(t),$$

$$\dot{z}(t) = \begin{bmatrix} -3 & 0 \\ 0 & -1 \end{bmatrix} z(t) + \begin{bmatrix} x(t) \\ \sin(x) \end{bmatrix} + \begin{bmatrix} 1 \\ 1 \end{bmatrix} u(t) + \begin{bmatrix} \sin(3t) \\ \cos(2t) \end{bmatrix},$$

$$\dot{p}(t) = \begin{bmatrix} -3 & 0 & 0 \\ 0 & -3 & 0 \\ 0 & 1 & -5 \end{bmatrix} p(t) + \begin{bmatrix} 1 \\ 1 \\ 1 \end{bmatrix} u(t) + \begin{bmatrix} -2.1 \\ 0.5 \\ 0.5 \end{bmatrix} q(t) + \begin{bmatrix} 7 + 0.2\sin(t) \\ 20 + 2\cos(3t) \\ 55 + 2\cos(6t) \end{bmatrix},$$

$$\dot{q}(t) = \begin{bmatrix} -3 & 0 & 0 \\ 0 & -1 & 0 \\ 0 & 0 & -4 \end{bmatrix} q(t) + \begin{bmatrix} 1 & 0 & 0 \\ 0 & 1 & 0 \\ 0 & 0 & 1 \end{bmatrix} p(t) + \begin{bmatrix} 1 \\ 1 \\ 1 \end{bmatrix} u(t) + \begin{bmatrix} 0.5\sin(3t) \\ 0.5\cos(2t) \\ 0.5\cos(2t) \end{bmatrix}.$$

The controller for this system has a $1ms$ time delay and is designed with the following parameters:

$$A_x = -5, \qquad B_x = 1, \qquad \omega = 50,$$

$$A_{p_1} = -4, \qquad B_{p_1} = 1,$$

$$A_{p_2} = -5, \qquad B_{p_2} = 1,$$

$$A_{p_3} = -6, \qquad B_{p_3} = 1,$$

with a time step of $T = 10^{-3}$. The limits for each of the three limiting states are

$$p_{1_{max}} = 5.5, \qquad p_{1_{min}} = 3,$$

$$p_{2_{max}} = 10, \qquad p_{2_{min}} = 7.5,$$

$$p_{3_{max}} = 15.1, \qquad p_{3_{min}} = 13.$$

In Figure 5 through Figure 7 the above system is seen with all six maximum and minimum limits being activated at 5 seconds.

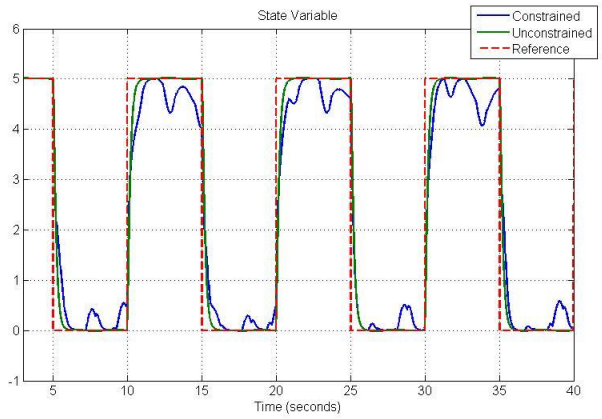

Figure 5: State $x(t)$ limited (blue) and unlimited (green)

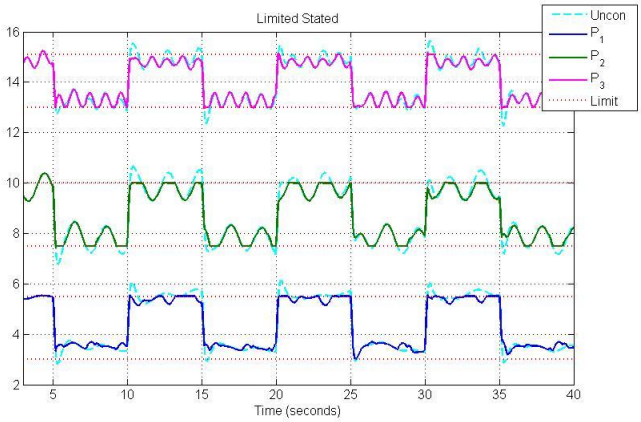

Figure 6: Limited $p(t)$, limited (blue, green, magenta), and unlimited (teal dashed)

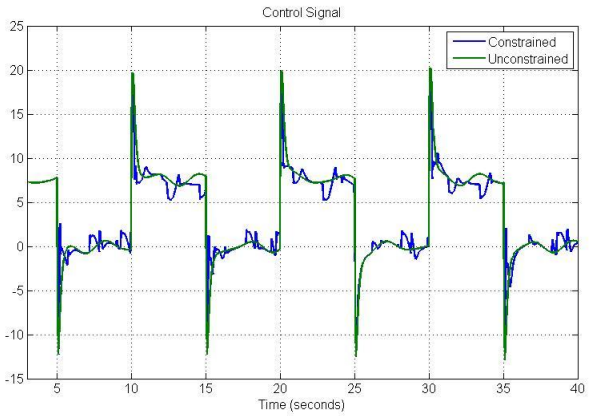

Figure 7: Control Signal $u(t)$, limited (blue), and unlimited (green)

The state variable $x(t)$ is shown in Figure 5. It is seen that both the unconstrained system (solid green line) and the constrained system (solid blue line) track the reference command (dashed red line). Again the constrained system does show some deterioration in its ability to follow the reference command, however, as seen in Figure 6, this is due to the constrained system holding each of the six limits. For the three $p_i(t)$ systems the limits, seen as red dotted lines, are held for the minimum and maximum values. Also, seen in Figure 7, the control signal, $u(t)$ is observed for both the constrained (blue line) and unconstrained (green line) system. The constrained control signal is shown to have more oscillations as compared with the unconstrained system, due to the switched between the state variable and the limited variable, as limits are reached. Although performance is reduced, the ability to indefinitely hold limits is worthwhile, as will been seen in the next section.

7. Application on Aircraft Engine

A. C-MAPSS40k

To further evaluate the $\mathcal{L}_1$ adaptive dynamic constraint theory the architecture is tested for an aircraft engine application. In this section $\mathcal{L}_1$ adaptive control is applied to a simulation model of a turbofan engine. The Commercial Modular Aero-Propulsion System Simulator Version 40k (CMAPSS40k) is a generic transient simulation representing a twin-spool, high bypass turbofan engine in the 40,000 lbf. thrust range[37]. The simulation is modeled in Simulink/Matlab (diagrams are found the Appendix), and consists of three main components: an engine model, a baseline controller, and an atmospheric model.

There are several main components which comprise the engine model: inlet, fan, bypass duct, bypass nozzle, low pressure compressor (LPC), high pressure compressor (HPC), burner, high pressure turbine (HPT), low pressure turbine (LPT) and core nozzle. Breaking down further, the fan includes two components, the fan tip, which allows flow to the bypass duct and nozzle, and the fan-hub, which allows flow to the LPC. For system accuracy, flow rate errors are balanced through each component every time step. However, to assure proper response to transient maneuvers, high and low rotor shaft torques are not balanced.

C-MAPSS40k contains its own control system. For this paper the control system will be referred to as "baseline." The baseline controller is a form of PID control and is meant to model control systems currently used in industry for commercial aircraft engines. The controller works by determining the fuel flow rate (lb/sec) necessary to achieve or

maintain the desired thrust level for a given environmental state. The desired thrust is based on the user-defined Power-Lever Angle (PLA). Three different user defined control modes can be utilized, EPR (engine pressure ratio), Fan speed (N_1), or Core Speed (N_2). For the purposes of this paper, fan speed is used and the controller will drive the fan speed to the reference value.

To ensure engine stability, safety, and life-time limits, constraints are applied based on structural and operation considerations (e.g., the fan speed must remain below some critical threshold). The baseline controller in C-MAPSS40k is a digital min-max controller based on these constraints.

This baseline controller will be used to evaluate the $\mathcal{L}_1$ adaptive controller. As seen in Figure 8, the model will run with either the baseline controller or the $\mathcal{L}_1$ adaptive controller. In the results section that is to follow, simulations are first run with the baseline controller and then the $\mathcal{L}_1$ adaptive controller under the same operating conditions, allowing for comparison between the two control designs.

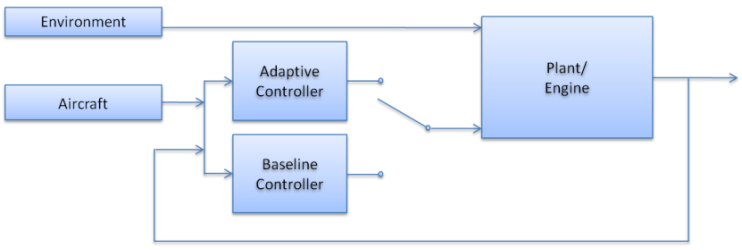

Figure 8: C-MAPSS40k Implementation

The baseline controller and atmospheric model supply the inputs for the engine model. The mass flow rate is determined via the baseline controller, which it interprets from the user defined throttle position. To characterize the operating environment for the engine, the atmospheric model takes into account the user defined Altitude (ATL), air

speed Mach Number (MN) and ambient air temperature minus the standard day temperature (dTamb). Outputs from the engine model are analyzed in Matlab.

The user is able to define the overall health of the engine to change the internal dynamics. A new healthy engine is characterized using a value of 0 for deterioration. A value of 1 corresponds to an engine at the end of its life cycle. Any value between 0 and 1 may be chosen to represent an indicative deterioration level.

B. Engine Limits

Although there are countless components to an engine, each having its own respective limit, only a handful of critical limits are monitored closely. Rotor speeds and burner pressure are the most critical limits to controlling the life of the engine and are often regulated. Surge and stall are avoided by controlling the acceleration of the rotor. C-MAPSS40k includes a novel surge/stall margin estimator, via a complex agglomeration of simple signals, to approximate the probability that the engine is not in a stall or surge.

Most state limits are single sided. As an example, the rotor may have a set maximum speed but lacks a certain minimum speed. Also, the surge/stall margin cannot go below 0% (meaning the probability of the engine not being is surge/stall is 0%), but this margin does not have an upper limit.

For this study the limits that will be controlled are: stall margin, maximum core rotor speed; minimum and maximum burner pressure (P30); the acceleration schedule $\left(\frac{dN_c}{dt}/N_c\right)$; and the fuel flow over burner pressure ratio (RU, Ratio Units). These limits were decided on based on the baseline controllers choice of the same limits.

C. Stall Margin Development

As mentioned previously, CMAPSS40k contains a novel stall margin estimator. In the specific application of turbofan control, the formulation of each constraint should be customized, specifically the stall margin constraint in which a stall margin limiter is developed. In the past [38], the stall margin has been shown to be the most difficult limit to control and new algorithms have been developed for its implementation. Therefore the following gives special attention to the stall margin constraint.

As discussed in Section 4, the constraint variables, $p_i(t)$, are implement as the integration limits in the control law. However, the stall margin state is implemented in the form of dynamic limits. The block diagram in Figure 9 shows the control architecture used to implement the $\mathcal{L}_1$ adaptive controller onto CMAPSS40k.

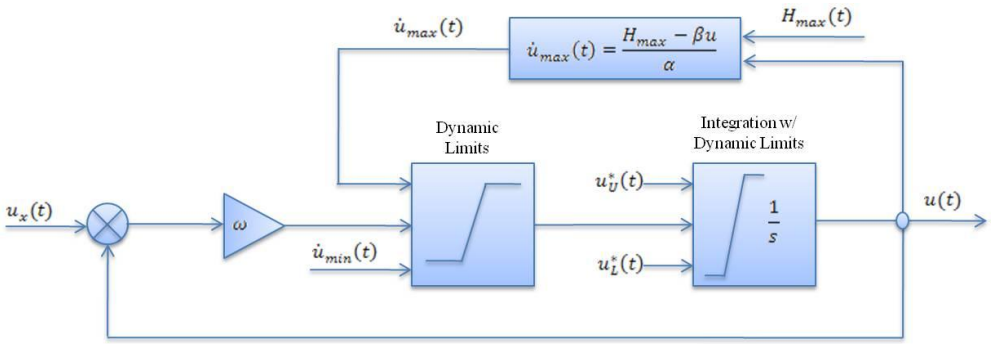

Figure 9: Dynamics of Control Law

The control architecture seen above takes the error between the reference control signal, $u_x(t)$ and the plant input control signal, $u(t)$ and then filters this signal. Next the signal is dynamically limited by $\dot{u}_{max}(t)$ and $\dot{u}_{min}(t)$. The signal is then integrated through the dynamic limiting described in Section 4. The two limits, $\dot{u}_{max}(t)$ and $\dot{u}_{min}(t)$ are a function of the stall margin and are developed in the following section.

The stall margin is dependent on the rate of change of fuel flow, as well as its value, therefore to apply the constraint a combination of these two factors is utilized. The value of the stall margin, $p(t)$ is assumed to be roughly related to the fuel flow, $u(t)$, by the following equation:

$$p = \alpha\dot{u} + \beta u + \gamma + \int \sigma_P,$$

(92)

where α, β, and γ are constant coefficients that relate fuel flow and its rate of change to the stall margin. The amount of error for this rough estimation of stall margin is considered by the term $\int \sigma_P$. As a result, the estimated value of stall margin would be:

$$\hat{p} = \alpha\dot{u} + \beta u + \gamma + \int \hat{\sigma}_P \; + A_{sm} \int \tilde{p}$$

(93)

where $\hat{\sigma}_P$ is the estimated value of σ_p and $\tilde{p} = \hat{p} - p$. Therefore the error dynamic is

$$\tilde{p} = \int \hat{\sigma}_P \; + A_{sm} \int \tilde{p}$$

(94)

Based on the error dynamic and to satisfy the constraint, $p < p_{max}$, the adaptation law becomes

$$\hat{\sigma}_P(t) = -\left(A_{sm} + \frac{1}{T}\right)\tilde{p}$$

(95)

which results in:

$$\alpha\dot{u} + \beta u < H_{max}$$

(96)

where H_{max} is the maximum value of $\alpha\dot{u} + \beta u$ before it reaches the limit and can be found as:

$$H_{max} = p_{max} - \int \hat{\sigma}_P \; - A_{sm} \int \tilde{p} - \gamma$$

(97)

In order to apply this constraint, it will be transformed to a constraint on $\dot{u}(t)$ such that

$$\dot{u}_{max}(t) = \frac{H_{max} - \beta u}{\alpha}$$

(98)

Therefore, the stall margin constraint is implemented in the form of the rate limit, $\dot{u}_{max}(t)$ and $\dot{u}_{min}(t)$ is set as a constant. Additionally, it is noted the smooth transition technique applied in (30)-(31) is similarly applied to $\dot{u}_{max}(t)$.

8. Results

Multiple simulations were run to show $\mathcal{L}_1$control in aircraft engine applications. In the following, simulations are presented to show the main capabilities of the $\mathcal{L}_1$controller developed in this thesis, namely its ability to respond faster, hold the stall margin limit, as well as hold multiple other limits. For the simulations that follow the performance of the $\mathcal{L}_1$controller is compared with the baseline controller and limit holding is analyzed.

A. Small Thrust Change

One of the benefits of $\mathcal{L}_1$control theory is its ability for fast adaptation. This feature can be useful in emergency situations were small thrust changes can be used to maneuver the aircraft. Therefore, in the first scenario, a small thrust change is observed, as seen in Figure 10 - Figure 12. Here the change in thrust is 270 lbf and is achieved by changing the initial PLA of 60 degrees to a PLA of 60.4 degrees at 30 seconds. The environmental conditions are set at a Mach Number of 0.3, a dTamb of 0 °F, and an altitude of 0 feet, with no engine deterioration. Note again that dTamb is the ambient air temperature minus the standard day temperature.

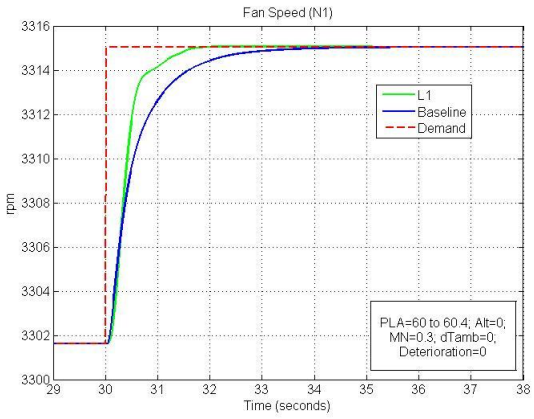

Figure 10: Small Thrust Change Fan Speed Command

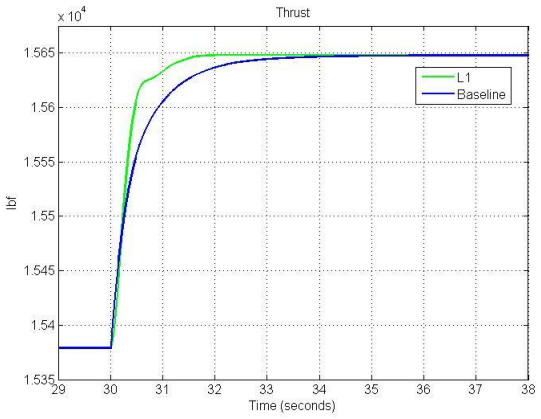

Figure 11: Small Thrust Change

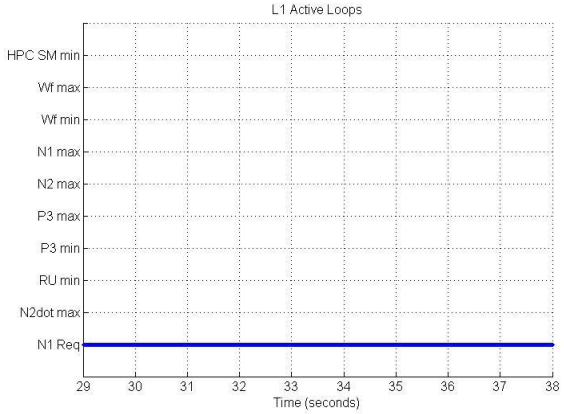

Figure 12: Small Thrust Change Control Signal Loop Activated

Figure 10 shows that $\mathcal{L}_1$ achieves a much faster response and settling time when compared with the baseline controller. $\mathcal{L}_1$ has a rise time of 0.54 seconds and a settling time of 1.10 seconds, while the baseline has a rise time of 1.29 seconds and a settling time of 1.90 seconds.

In order to show if limits are active Figure 12 was created to show which control signal is activated at a given time. As expected for such small changes in thrust, no limits are reached, as evident in Figure 12. Here it is seen that the only control loop activated is the reference loop, N_1 (fan speed).

To further show $\mathcal{L}_1$ adaptive control achieves a faster response, a small thrust change is again used. However, in this scenario harsher operating conditions are used (Figure 13 - Figure 15). The thrust change of 250 lbf, seen in Figure 14, is achieved by changing the PLA from 52 degrees to 52.4 degrees. The engine is an end of life engine. The dTamb is 20 °F, at an altitude of 5000 feet, and at a Mach Number of 0.4.

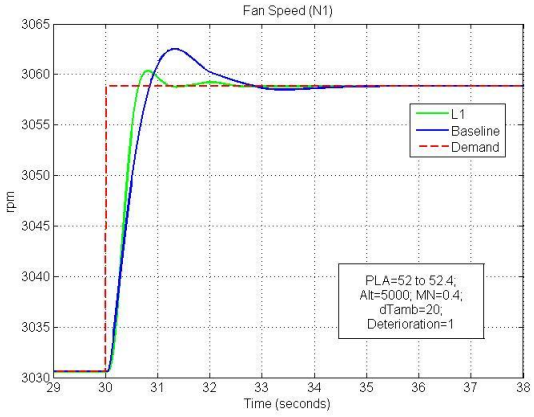

Figure 13: Small Thrust Change on End of Life Engine Fan Speed Command

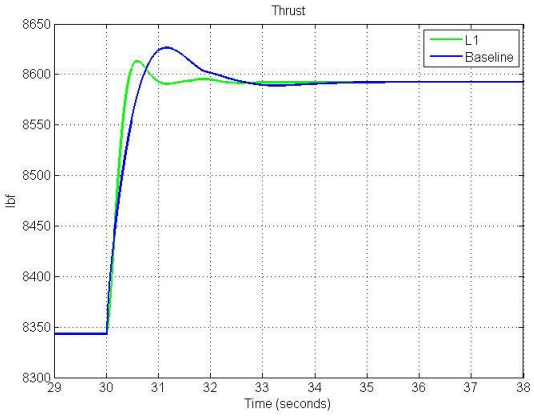

Figure 14: Small Thrust Change on End of Life Engine

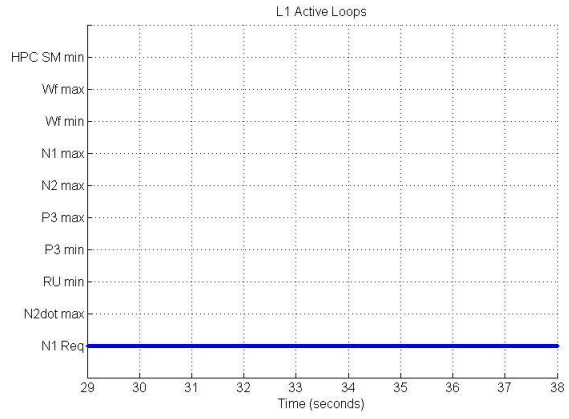

Figure 15: Small Thrust Change on End of Life Control Signal Loop Activated

Once again, even in harsh operating conditions $\mathcal{L}_1$ still has a faster response as seen in Figure 13 and again for the small thrust changes no limits are active, as visible in Figure 15.

B. Stall Margin Limited

As mention previously, the stall margin limit was specially developed. Therefore the next set of scenarios is devoted to looking at $\mathcal{L}_1$'s ability to maintain this stall margin limit. Here a "worst case" scenario is seen where the PLA is set to go from idle to maximum acceleration (Figure 16 - Figure 19). The engine is an end of life engine, the temperature is set to be a "hot day" at 88°F and the altitude is 10,000 feet.

Figure 16 shows $\mathcal{L}_1$ reaching the reference signal faster than the baseline controller. Also in this set of simulations it is seen that the stall margin limit of 0% is reached, as evident in Figure 18 and Figure 19.

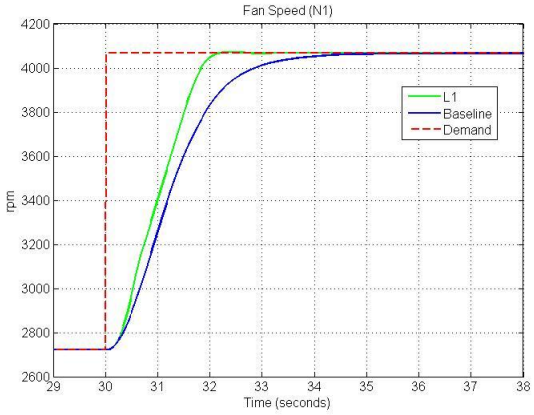

Figure 16: Stall Margin 0% Limit Fan Speed Command

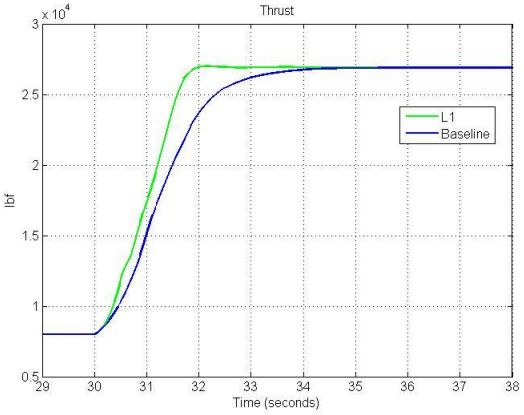

Figure 17: Stall Margin 0% Limit Thrust Change

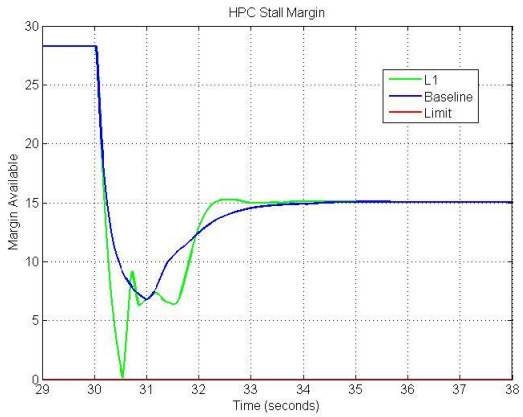

Figure 18: Stall Margin Limit 0%

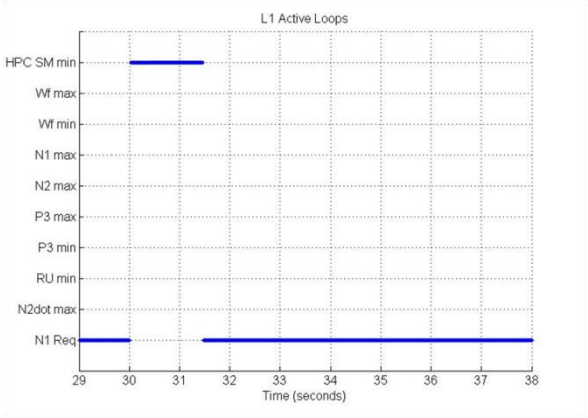

Figure 19: Stall Margin 0% Limit Control Signal Loop Activated

In the simulation above the stall margin is set to the default 0% and for a few seconds this limit is hit and the control loop switches to the stall margin limit loop. To further show the capabilities of $\mathcal{L}_1$ stall margin limit holding, using the same conditions as above, the stall margin limit is increased to 10%, as seen in Figure 20 to Figure 23.

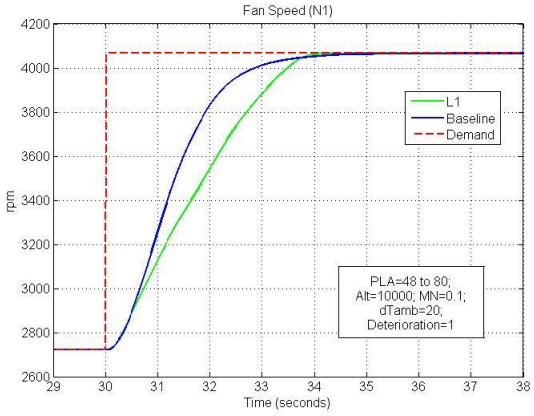

Figure 20: Stall Margin 10% Limit Fan Speed Command

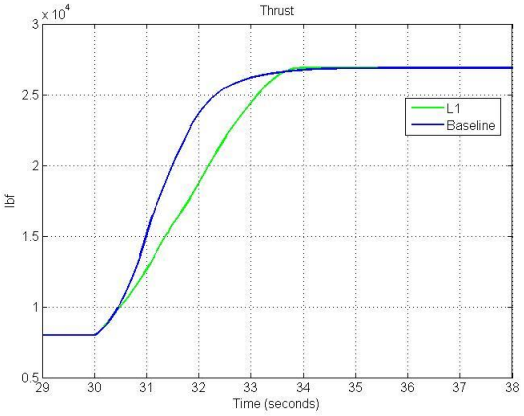

Figure 21: Stall Margin 10% Limit Thrust Change

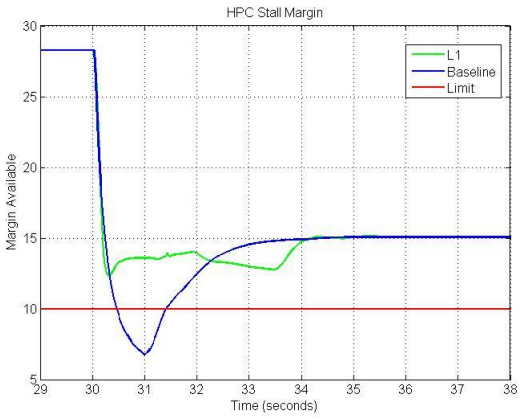

Figure 22: Stall Margin Limit 10%

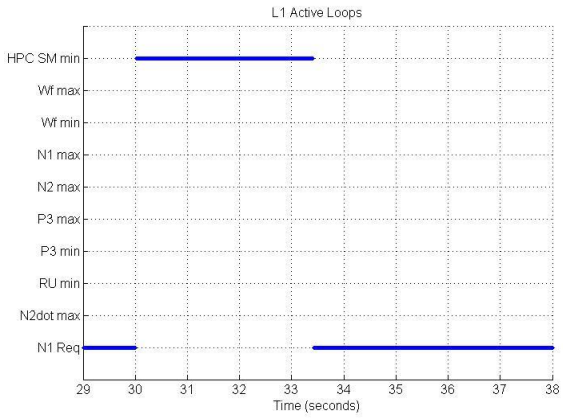

Figure 23: Stall Margin 10% Limit Control Signal Loop Activated

Figure 20 shows that $\mathcal{L}_1$ does not achieve a faster response than the baseline. This is due to the trade-off between limit holding and performance. As Figure 22 shows $\mathcal{L}_1$ keeps the stall margin above the set 10% limit and the stall margin control signal is the active control loop as seen in Figure 23.

C. Multiple Limit Holding

Finally, the $\mathcal{L}_1$ control architecture designed in this paper has the ability to hold multiple limits. In order to show multiple limit holding, more conservative limits are implemented to ensure the different control channels will be activated. For Figure 24 to Figure 31, the following limits are utilized: maximum core rotor speed is reduced from 12,200 to 10,420 rpm's; maximum burner pressure is reduced from 433 to 200 psi; the ratio between fuel flow and burner pressure is increased from 17 to 20; and the minimum burner pressure limit is increased from 53 to 155 psi.

First, an acceleration case is seen to show the maximum limits are held and than a deceleration scenario is seen for the minimum limit holding. In both scenarios the operating conditions are set at an altitude of 5000 feet, a Mach Number of 0.2, and dTamb of 0°F, with no engine deterioration. It is noted that the baseline controller is not

observed in the following cases. While the baseline control does have some limiting logic built-in, the model does not handle such conservative limits applied. Therefore, the baseline control cannot be used as an accurate metric for comparing of the two different controllers.

Figure 24 shows the acceleration case were PLA changes from 49 to 52 degrees at 30 seconds. In this scenario the maximum core rotor speed loop is activated as well at the burner pressure maximum.

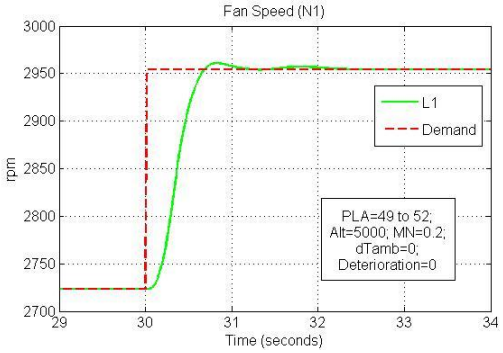

Figure 24: Multiple Limits Accel Fan Speed Command

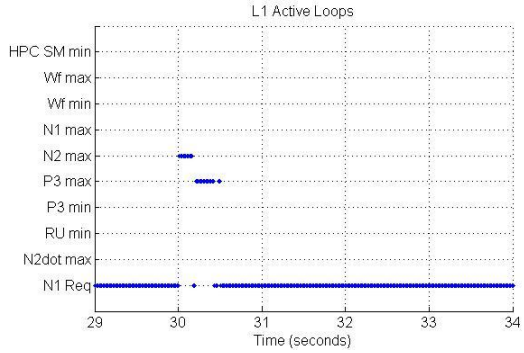

Figure 25: Multiple Limits Accel Control Signal Loop Activated

Figure 26 and Figure 27 show that while the control signal was in the core rotor speed and burner pressure loops, respectively neither limit was exceeded.

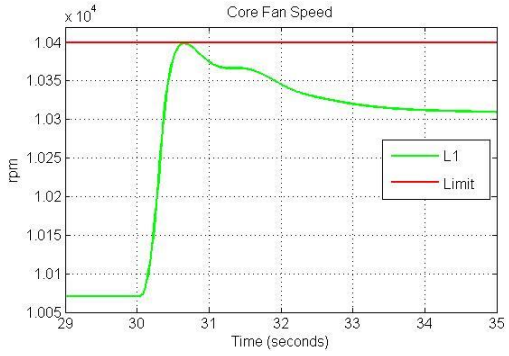

Figure 26: Multiple Limits Accel Core Rotor Speed

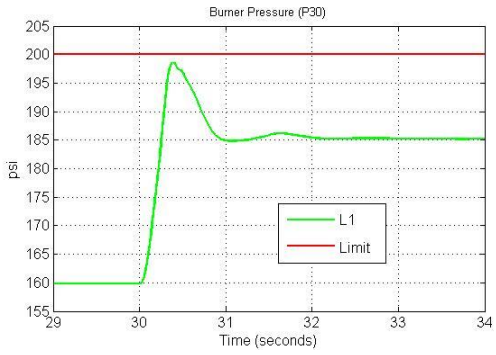

Figure 27: Multiple Limits Accel Burner Pressure

Next, using the same operating conditions a deceleration scenario is obseved, this time using a PLA change of 52 to 49 degrees (the reverse of the above case). Figure 28 shows a slower response time of about 3 seconds, however this is due to the two minimum limits being reached and the control signal switching to the respective control channels as seen in Figure 29. While the control loops are activated for RU minimum and the minimum value for burner pressure, neither limit is exceed as seen in Figure 30 and Figure 31 respectively.

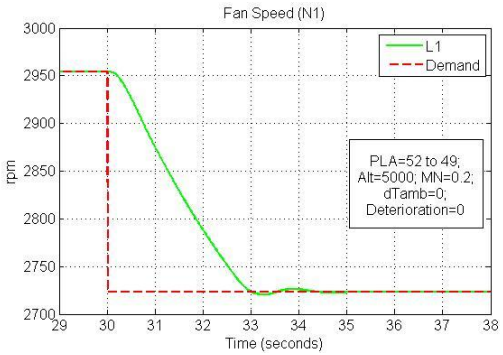

Figure 28: Multiple Limits Decel Fan Speed Command

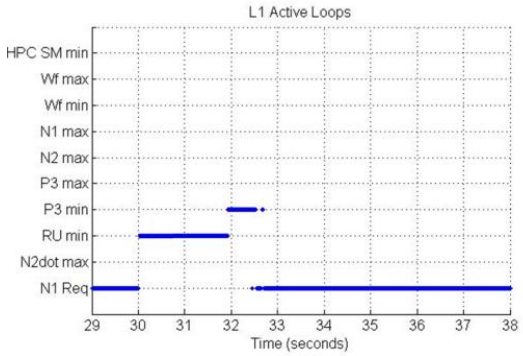

Figure 29: Multiple Limits Decel Control Signal Active Loop

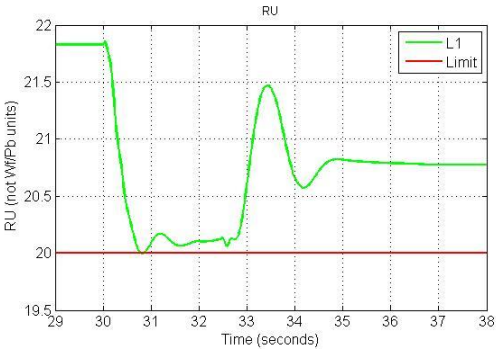

Figure 30: Multiple Limits Decel Ratio Units Limit

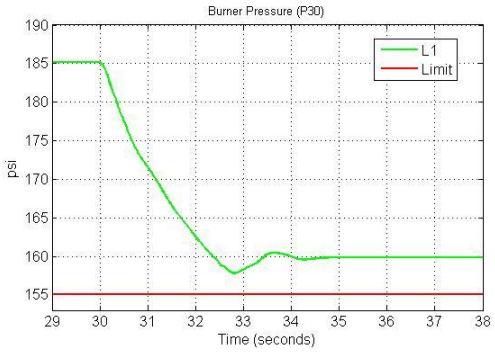

Figure 31: Multiple Limits Decel Burner Pressure Limit

9. Conclusion

A novel $\mathcal{L}_1$ adaptive control architecture was presented and shown to have bounded performance in the presence of multiple limits. The $\mathcal{L}_1$ adaptive control theory was theoretically developed to handle state constraints. Generic multiple limit simulations were shown to be valid. Constraint logic for the stall margin limit was specially developed and $\mathcal{L}_1$ adaptive control was applied to an aircraft engine simulation model. $\mathcal{L}_1$ was shown to have faster response time, as well as maintain prescribed limits.

In future endeavors, the work presented here could be extended in the following ways: First, a method could be created to prioritize limits and allow for limit dropping in emergency situations. Second, $\mathcal{L}_1$ could be developed to use output feedback for the constraint systems and the theory could be extended to multiple-input multiple-output (MIMO) case. Third, optimal control could be incorporated into $\mathcal{L}_1$ theory to better handle the constraints. Finally, to make any adaptive commercial flight control viable, it must be certified by the FAA. Current certification procedures use metrics designed for linear controllers, such as gain and phase margin [39]. Such techniques cannot be used for nonlinear control designs. Therefore, new metrics must be developed so adaptive control can be certified for use in commercial aircraft engines.

Appendix

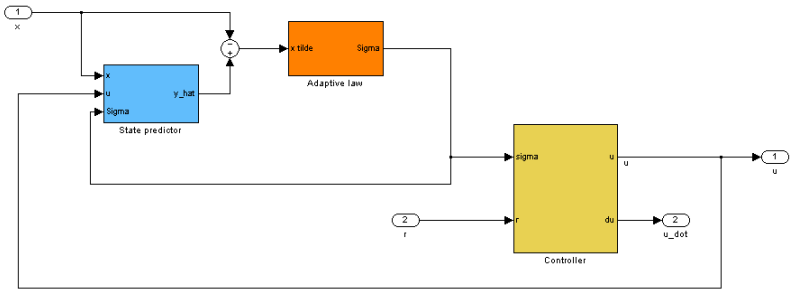

Figure 32: General $\mathcal{L}_1$ Structure Modeled in Simulink

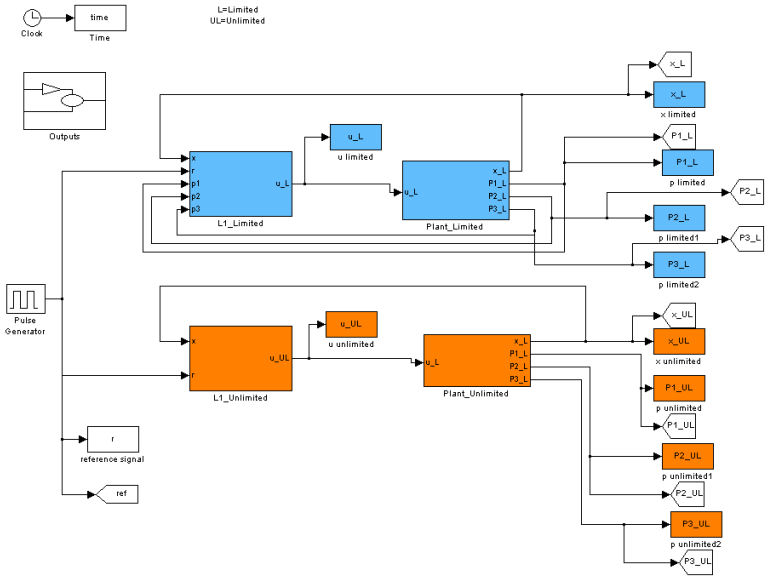

Figure 33: Top Level Simulink Model for Multiple Limit Simulation

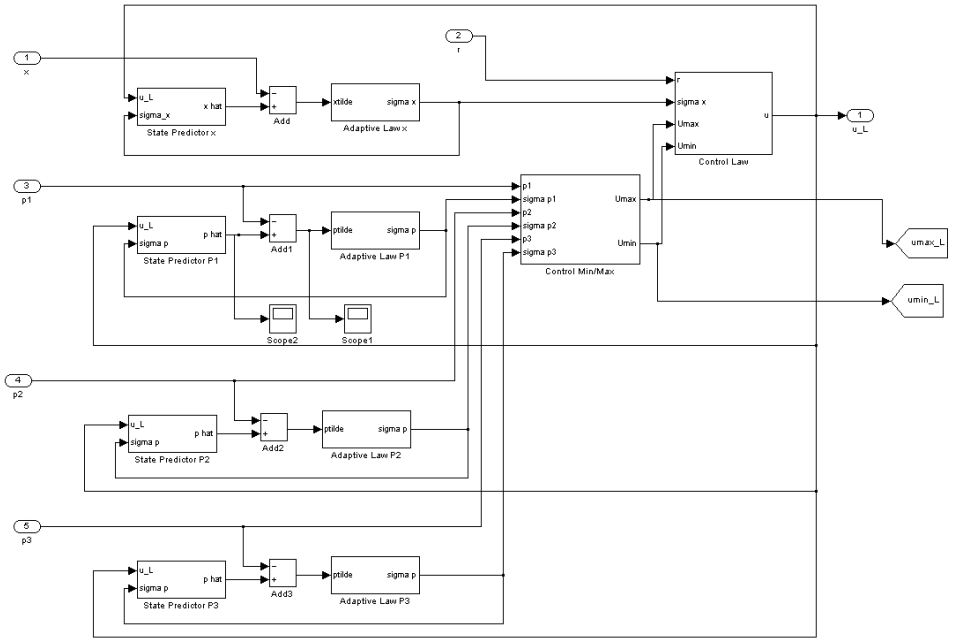

Figure 34: $\mathcal{L}_1$ Adaptive Controller Implemented on Multiple Limit Simulation

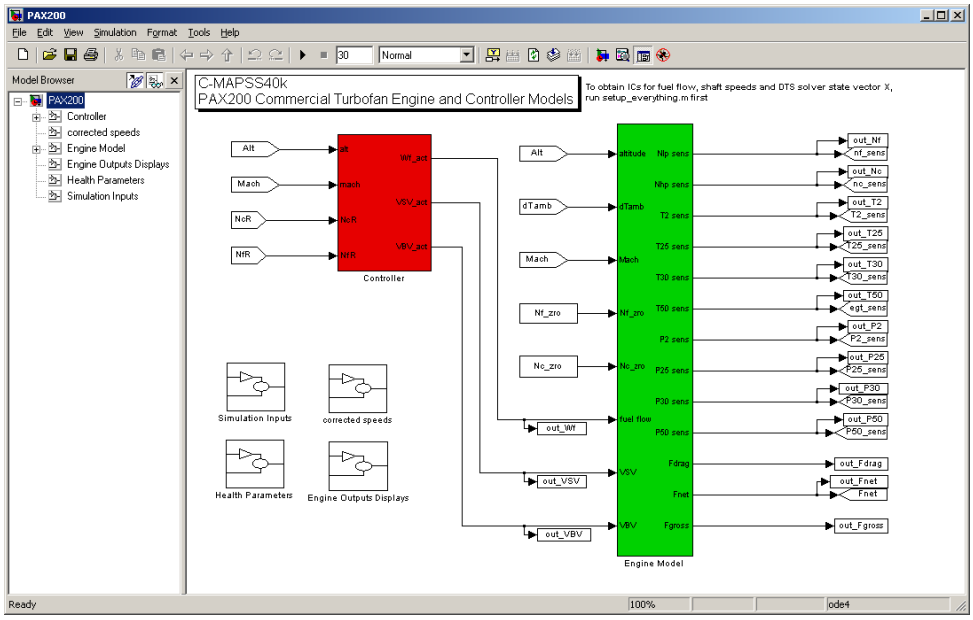

Figure 35: Simulink Model of NASA's C-MAPSS40k

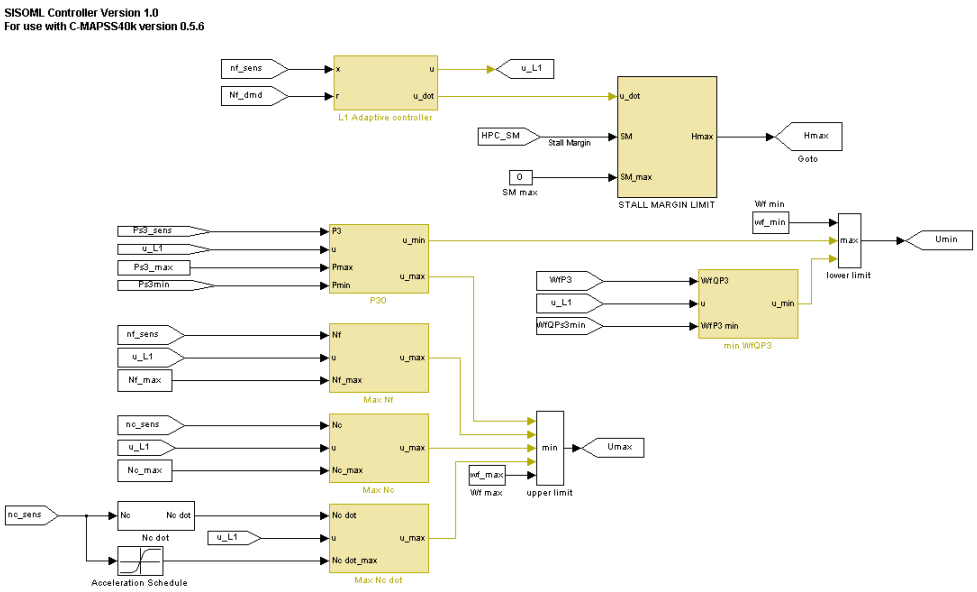

Figure 36: Top Level Simulink Model of $\mathcal{L}_1$ Controller Implemented on C-MAPSS40k

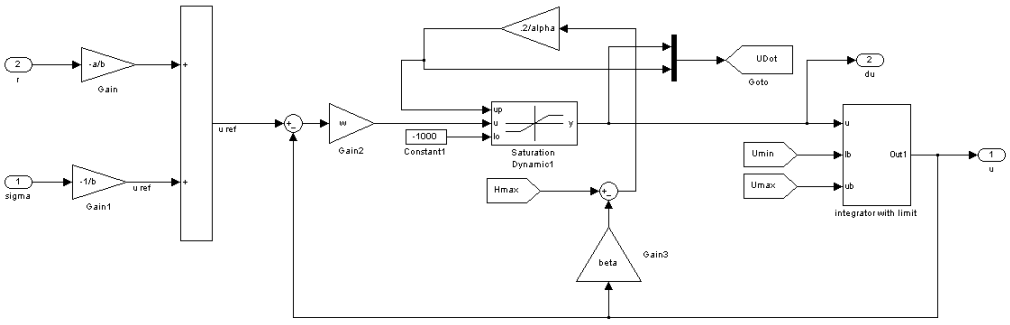

Figure 37: Simulink Model of $\mathcal{L}_1$ Control Law Implemented on C-MAPSS40k

References

[1] FAA, "Airworthiness Standards: Aircraft Engines: Subpart E–Design and Construction; Turbine Aircraft Engines," Federal Aviation Administration.
[2] Jaw, L. C., 2009, Aircraft Engine Controls: Design, System Analysis, and Health Monitoring, American Institute of Aeronautics and Astronautics, Inc., Reston, VA.
[3] Litt, J., Frederick, D. K., and Guo, T.-H., April 2009, "The Case for Intelligent Propulsion Control for Fast Engine Response," AIAA Infotech Aerospace ConferenceSeattle, Washington.
[4] Spang, H. A., and Brown, H., 1999, "Control of Jet Engines," Control Engineering Practice, 7(9), pp. 1043-1059.
[5] Levy, Y., and Lichtsinder, M., Oct 2006, "Jet Engine Model for Control and Real-Time Simulations," Journal of Engineering for Gas Turbines and Power, 128(4), pp. 745-753.
[6] Franklin, G. F., Powell, J. D., and Emami-Naeini, A., 2010, Feedback Control of Dynamic Systems, Prentice Hall, Upper Saddle River, NJ.
[7] Guo, T.-H., and Litt, J., May 2007, "Resilient Propulsion Control Research for the NASA Integrated Resilient Aircraft Control (IRAC) Project," AIAA Infotech Aerospace ConferenceRohnert Park, CA.
[8] National Transportation Safety Board. 2007, "Aircraft Accident Report: Attempted Takeoff from Wrong Runway Comair Flight 5191 Bombardier CL-600-2B19, N431Ca Lexington, Kentucky August 27, 2006," No. NTSB/AAR-07/05, PB2007-910406, Washington DC.
[9] Mayne, D. Q., Rawlings, J. B., Rao, C. V., and Scokaert, P. O. M., 2000, "Constrained model predictive control: Stability and optimality," Automatica, 36, pp. 789-814.
[10] Camacho, E. F., and Bordons, C., 2007, Model Predictive Control, Springer, London.
[11] Young, K. D., Utkin, V. I., and Ozguner, U., 1999, "A Control Engineer's Guide to Sliding Mode Control," IEEE Trans. on Control Systems Tech, 7(3), pp. 328-342.
[12] Plestan, F., Glumineau, A., and Laghrouche, S., 2008, "A new algorithm for high-order sliding mode control," INTERNATIONAL JOURNAL OF ROBUST AND NONLINEAR CONTROL, 18, pp. 441-453.
[13] Atassi, A. N., and Khalil, H. K., 1999, "A Separation Principle for the Stabilization of a Class of Nonlinear Systems," IEEE TRANSACTIONS ON AUTOMATIC CONTROL, 44(9), pp. 1672-1687.
[14] Krstic, M., Kanellakopoulos, I., and Kokotovic, P., 1995, Nonlinear and Adaptive Control Design, John Wiley & Sons, Inc., New York.
[15] Khalil, H. K., 2002, Nonlinear Systems, Prentice Hall, Upper Saddle River, New Jersey.

[16] Lee, C. C., 1990, "Fuzzy Logic in Control Systems: Fuzzy Logic Controller-Part I," IEEE Trans. on Systems, Man, and Cybernetics, 20(2), pp. 404-418.
[17] Hang, C., and Parks, P., 1973, "Comparative Studies of Model Reference Adaptive Control Systems," IEEE Trans. Automatic Control, 18(5), pp. 419-427.
[18] Yucelen, T., and Calise, A., April 2010, "Adaptive Control for the Generic Transport Model: a Derivative-Free Approach," AIAA Infotech Aerospace ConferenceAtlanta, Georgia.
[19] Dydek, Z. T., Annaswamy, A. M., and Lavretsky, E., 2008, "Adaptive Control and the NASA X-15 Program: A Concise History, Lessons Learned, ans a Provably Correct Design," American Control ConferenceSeattle, Washington.
[20] Hovakimyan, N., and Cao, C., 2010, L1 Adaptive Control Theory: Guaranteed Robustness and Fast Adaptation, SIAM, Philadelphia.
[21] Cao, C., and Hovakimyan, N., 2006, "Design and Analysis of a Novel L1 Adaptive Controller, Part I: Control Signal and Asymptotic Stability," American Control ConferenceMinneapolis, Minnesota, pp. 3397-3402.
[22] Cao, C., and Hovakimyan, N., 2006, "Design and Analysis of a Novel L1 Adaptive Controller, Part II: Guaranteed Transient Performance," American Control ConferenceMinneapolis, Minnesota, pp. 3403-3408.
[23] Cao, C., and Hovakimyan, N., 2007, "Guaranteed Transient Performance with L1 Adaptive Controller for Systems with Unknown Time-varying Parameters and Bounded Disturbances: Part I," American Control Conference New York City, pp. 3925-3930.
[24] Cao, C., and Hovakimyan, N., 2008, "L1 Adaptive Controller for Systems with Unknown Time-varying Parameters," International Journal of Control, 81(7), pp. 1147-1161.
[25] Cao, C., and Hovakimyan, N., 2008, "L1 Adaptive Controller for a Class of Systems with Unknown Nonlinearities: Part I," American Control ConferenceSeattle, Washington, pp. 4093 - 4098
[26] Cao, C., and Hovakimyan, N., 2008, "Design and Analysis of a Novel L1 Adaptive Control Architecture with Guaranteed Transient Performance," IEEE Trans. on Automatic Control, 53(2), pp. 586–591.
[27] Cao, C., and Hovakimyan, N., 2008, "L1 Adaptive Controller for Nonlinear Systems in the Presence of Unmodelled Dynamics: Part II," American Control Conference Seattle, Washingtion, pp. 4099-4104.
[28] Cao, C., and Hovakimyan, N., 2008, "L1 Adaptive Controller for Multi-Input Multi-Output Systems in the Presence of Unmatched Disturbances," American Control Conference Seattle, WA, pp. 4105-4110.
[29] Cao, C., and Hovakimyan, N., 2008, "L1 Adaptive Output Feedback Controller for Non Strickly Positive Real Reference Sysstems with Applications to Aerospace Examples," AIAA Guidance, Navigation and Control ConferenceHonolulu, Hawaii.
[30] Merrill, W., Van, H. T., and Mink, G., April 2010, "Fast Engine Response for Emergency Aircraft Operation," AIAA Infotech Aerospace ConferenceAtlanta, Georgia.
[31] Litt, J., Sharp, L., and Guo, T.-H., April 2010, "A Risk Assessment Architecture for Enhanced Engine Operation," AIAA Infotech Aerospace ConferenceAtlanta, Georgia.
[32] Li, Z., Hovakimyan, N., Cao, C., and Kaasa, G.-O., 2009, "Integrated Estimator and L1 Adaptive Controller for Well Drilling Systems," American Control ConferenceSt. Louis, MO, pp. 1958 - 1963.

[33] Kharisov, E., and Hovakimyan, N., April 2010, "Application of L1 Adaptive Controller to Wing Rock," AIAA Infotech Aerospace ConferenceAtlanta, GA.
[34] Gregory, I. M., Cao, C., Xargay, E., Hovakimyan, N., and Zou, X., 2009, "L1 Adaptive Control Design for NASA AirSATR FLight Test Vehicle," AIAA Guidance, Navigation, and Control ConferenceChicago.
[35] Gudeman, K., 2010, "Nice Recovery! Pilots get help saving uncontrollable aircraft," http://engineering.illinois.edu/news/.
[36] Kreyszig, E., 2006, Advanced Engineering Mathematics, 9th ed, John Wiley and Sons Inc., Hoboken, NJ.
[37] May, R. D., Csank, J., Litt, J. S., and Guo, T.-H., 2010, "Commercial Modular Aero-Propulsion System Simulation 40k (C-MAPSS40k) User's Guide," NASA Glenn Research Center, Cleveland, OH.
[38] Thompson, A., Hacker, J., and Cao, C., April 2010, "Adaptive Engine Control in the Presence of Output Limits," AIAA Infotech Aerospace ConferenceAtlanta, Georgia.
[39] Larchev, G., Campbell, S., and Kaneshige, J., April 2007, "Projection Operator: A Step Towards Certification of Adaptive Controllers," AIAA Infotech Aerospace ConferenceAtlanta, Georgia.